Supplementary Information for

FOXA1 overexpression suppresses interferon signaling and immune response in cancer

Yundong He, Liguo Wang, Ting Wei, Yu-Tian Xiao, Haoyue Sheng, Hengchuan Su, Daniel P. Hollern, Xiaoling Zhang, Jian Ma, Simeng Wen, Hongyan Xie, Yuqian Yan, Yunqian Pan, Xiaonan Hou, Xiaojia Tang, Vera J. Suman, Jodi M. Carter, Richard Weinshilboum, Liewei Wang, Krishna R. Kalari, Saravut J. Weroha, Alan H. Bryce, Judy C. Boughey, Haidong Dong, Charles M. Perou, Dingwei Ye, Matthew P. Goetz, Shancheng Ren and Haojie Huang

This PDF file includes:

Supplementary Methods

Cell lines and cell culture

LNCaP, VCaP, DU145, PC3, NCI-H660, MCF7, MDA-MB-231, RT4, TRAMP-C2, MyC-CaP and 293T cell lines were purchased from ATCC. LNCaP, VCaP and PC3 cells were maintained at 37°C and 5% CO2 in RPMI 1640 containing 10% fetal bovine serum (FBS) and 1% antibiotic/antimycotic (Thermo Fisher Scientific). NCI-H660 cells were maintained at 37°C in HITES medium (RPMI1640 medium plus 0.005mg/ml Insulin, 0.01mg/ml Transferrin, 30nM Sodium selenite, 10nM Hydrocortisone, 10nM beta-estradiol and 2mM L-glutamine) with 10% FBS and 1% antibiotic/antimycotic (Thermo Fisher Scientific). MCF7, DU145, TRAMP-C2, MyC-CaP and 293T cells were maintained in DMEM medium with 10% FBS. MDA-MB-231 cells were maintained at 37°C and 5% CO2 in Leibovitz's L15 containing 10% fetal bovine serum (FBS) and 1% antibiotic/antimycotic (Thermo Fisher Scientific). RT4 cells were maintained at 37°C and 5% CO2 in McCoy's 5a containing 10% fetal bovine serum (FBS) and 1% antibiotic/antimycotic (Thermo Fisher Scientific). Mycoplasma contamination was tested by the PCR Mycoplasma Detection Set (Takara, Otsu, Japan). All cell lines are negative for mycoplasma contamination.

RNA-seq analyses and real-time PCR

For RNA-seq, libraries were prepared using Illumina TruSeq RNA prep kit and standard protocol. The RNA libraries were sequenced as 51 nt pair-end reads at one sample per lane of an Illumina HiSeq 4000, generating an average of 265 million reads per sample. All reads were aligned to the human reference genome (hg19/GRCh37) by TopHat 2.0.9 using default options. Gene expression counts were generated using RSeQC and expression differential analysis was conducted using edgeR (version 3.6.8) (1). Differentially expressed genes were determined based on the false discovery rate (FDR) threshold 1e-5 and log2 fold change threshold of 1.0. The Gene ontology biological process (GO-BP) analysis was performed by gene set enrichment analysis online (http://software.broadinstitute.org/gsea/msigdb/annotate.jsp) (2, 3). For RT-PCR, cells treated with or without 100 ng/L IFNα (SigmaAldrich, # I4276) for 24 h were harvested for RNA extraction using Trizol Reagent (Thermo Fisher Scientific, # 15596018). RNA was eluted in RNase-Free H_2O and reverse-transcribed to cDNA following the manufacturer's protocol (Thermo Fisher Scientific, # FERK1672). Gene expression was determined by qPCR using

Power SYBR Green (Thermo Fisher Scientific, # 4368708). Primer sequences used for RT-qPCR are listed in Supplementary Table 4.

Luciferase reporter assay for interferon (IFN)-stimulated response activity

To analyze the interferon-stimulated response activity, cells were transfected using lipofectamine 2000 (Invitrogen) according to the manufacturer's instructions with the following plasmids: interferon-stimulated response element luciferase reporter (ISRE-luc, purchased from Promega) containing type I and III IFN response elements, IFN-γ-activated sequence luciferase reporter (GAS-luc, a gift from Dr. Avudaiappan Maran at Mayo Clinic) (4) containing type II IFN response elements, Renilla-luc (phRL-TK, purchased from Promega) as internal control reporter, FOXA1-WT or FOXA1 mutants. At 24 h after transfection, the cells were treated with 100 ng/L IFNα (Sigma-Aldrich, # I4276) or IFNγ (Sigma-Aldrich, # SRP3058) for 5 hours. Renilla and firefly activities were measured with luminometry using the Dual-Luciferase Reporter Assay System (Promega) and the ratio was calculated. Results were shown as the ratio of firefly over Renilla luciferase activity.

Plasmid construction and mutagenesis

Wild-type (WT) V5-tagged FOXA1 lentiviral plasmid was purchased from Addgene (# 70090) and cloned into the SFB-tagged pcDNA3.1 or Flag-tagged pcDNA3.1 or pTSIN lentiviral vector using Phusion High-Fidelity DNA Polymerase (New England Biolabs, # M0530L). FOXA1 hotspot mutations (H247Q, R261G and F266L) and FOXA1 truncation mutations were engineered from FOXA1-WT using the KOD-Plus-Mutagenesis Kit (TOYOBO, # KOD-201) according to the manufacturer's instructions. To generate theFOXA1 luciferase reporter (FOXA1-luc) construct, six copies of the FOXA1 response element from the *KLK3* (PSA) gene 5'-tcgaTGTTTACTTAcagtaTGTTTACTTTatccgTGTTTACATAgtctaTATTTACTTAccataTGTTTGCTTAgtcaTGTTTACTCA-3' were inserted into pGL4.28 luc2CP/minP/hygro (Pomega). All plasmids were confirmed using Sanger sequencing. Mutant plasmids were further transfected in 293T cells to confirm the expression of the mutant proteins.

Cell transfection and RNA interference

293T cells were co-transfected with pTSIN-Vector or pTSIN-FOXA1 WT or mutant lentiviral plasmids along with packaging and envelope plasmids by Lipofectamine 2000 according to the manufacturer's instructions. At two days post-transfection, virus particles were used to infect cells according to the protocol provided by Sigma-Aldrich. The interest cells were infected with a 1:1 mixture of fresh medium and virus supernatant supplemented with Polybrene (4 μg/ml final concentration) for 24 h. To knock down FOXA1, cells were transfected using Lipofectamine 2000 with 50 nM FOXA1 siRNA (5'-GAGAGAAAAAAUCAACAGC-3' (siFOXA1#1, at the 3' UTR region) or 5'-GCACUGCAAUACUCGCCUU-3' (siFOXA1#2, at the CDS region)) or siSTAT2 (L-012064-00-0005, Dharmacon) or non-targeting control siRNA (siCon) 5'-UAGCGACUAAACACAUCAA-3' (synthesized from Dharmacon). For inducible shFoxa1 construction, the shRNA sequence against Foxa1 (shFoxa1#1 sense: 5'-TCGAGTGCCTTCTCAATGTTAATTTACTCGAGTAAATTAACATTGAGAAGGCATTTTTG-3'; shFoxa1#1 antisense: 5'-AATTCAAAAATGCCTTCTCAATGTTAATTTACTCGAGTAAATTAACATTGAGAAGGCA-3'; shFoxa1#2 sense: 5'-TCGAGACTCTCCTTATGGCGCTACCCTCGAGGGTAGCGCCATAAGGAGAGTTTTTTG-3'; shFoxa1#2 antisense: 5'-AATTCAAAAAACTCTCCTTATGGCGCTACCCTCGAGGGTAGCGCCATAAGGAGAGTC-3') was cloned into the lentiviral doxycycline-inducible pINDUCER10 vector (5) using XhoI and EcoR I sites. Then lentiviral plasmids along with packaging and envelope plasmids by Lipofectamine 2000 according to the manufacturer's instructions. At two days post-transfection, virus particles were used to infect cells according to the protocol provided by Sigma-Aldrich. The MyC-CaP cells were infected with a 1:1 mixture of fresh medium and virus supernatant supplemented with Polybrene (4 μg/ml final concentration) for 24 h. The knockdown or transfection efficiency was determined using Western blotting analysis.

Western blot

The cells were lysed and equal amounts of protein (50–100 μg) from cell lysate were denatured in sample buffer (#NP0007, Thermo Fisher Scientific), subjected to SDS-polyacrylamide gel electrophoresis (PAGE), and transferred to nitrocellulose membranes (Bio-Rad). The membranes were immunoblotted with specific primary antibodies, horseradish peroxidase (HRP)-conjugated

secondary antibodies, and visualized by SuperSignal West Pico Stable Peroxide Solution (# 34577, Thermo Fisher Scientific). The primary antibodies used in this study include AR (dilution 1:1000; #sc-816, Santa Cruz Biotechnology), FOXA1 (dilution 1:2000; # ab23738, Abcam), FOXA1 (dilution 1:1000, # sc-101058, Santa Cruz Biotechnology), FOXA2 (dilution 1:1000; #8186, Cell Signaling Technology), FOXA3 (dilution 1:500, # sc-74424, Santa Cruz Biotechnology), STAT1 (dilution 1:1000; #14994S, Cell Signaling Technology), STAT2 (dilution 1:1000; # 72604S, Cell Signaling Technology), Phospho-STAT1 (Tyr701) (dilution 1:1000; # 9167S, Cell Signaling Technology), Phospho-STAT2 (Tyr690) (dilution 1:1000; # 88410S, Cell Signaling Technology), IRF9 (dilution 1:1000; # 76684S, Cell Signaling Technology), ISG15 (dilution 1:500; # sc-166755, Santa Cruz Biotechnology), PARP1 (dilution 1:1000; # 9532S, Santa Cruz Biotechnology), HSP70 (dilution 1:1000; #4873S, Santa Cruz Biotechnology), MHC class I (MHC-I) (dilution 1:500; # sc-55582, Santa Cruz Biotechnology), Flag (dilution 1:1000; # F1804, Sigma-Aldrich) and V5 (dilution 1:1000; # A190-120A, Bethyl Laboratories), HA (dilution 1:1000; # MMS-101R, Covance), HDAC2 (dilution 1:1000; # sc-7899, Santa Cruz Biotechnology) and ERK2 (dilution 1:2000; # sc-1647, Santa Cruz Biotechnology).

Co-immunoprecipitation (co-IP), protein purification and GST pulldown assay

The NE-PER Nuclear and Cytoplasmic Extraction Kit (# 78835, Thermo Fisher Scientific) was used for extraction of nuclear and cytoplasmic proteins from cells according to the manufacturer's instruction. For extraction of whole cell lysate, we used IP buffer (50 mM Tris-HCl pH7.5, 150 mM NaCl, 1% NP40, 0.5% Sodium Deoxycholate). Protein A/G agarose (# 20421, Thermo Fisher Scientific) was used for immunoprecipitation of FOXA1 (# ab23738, Abcam) and Flag-tag (# F1804, Sigma-Aldrich). Monoclonal anti-HA agarose (# A2095, Sigma-Aldrich) was used for HA-tag Co-IP. For glutathione-S-transferase (GST) pulldown assay, GST-tagged STAT2 fragment expressed at *E. coli* was purified by Glutathione Sepharose 4B beads (# 84-239, Genesee Scientific) and incubated with lysate from 293T cells expressing interested proteins or in vitro transcribed/translated proteins followed by GST pulldown assays. For protein co-IP, samples eluted in IP butter were incubated with agarose beads and antibodies overnight at 4 °C, followed by wash for 6 times with IP buffer in the following day. Samples were boiled for

10 min in 50 µl sample buffer (2% SDS, 10% glycerol, 10% β-mercaptoethanol, bromophenol blue and Tris-HCl, pH 6.8) and subjected to Western blotting analysis.

FOXA1 luciferase reporter assay and electrophoretic mobility shift assay (EMSA)

For FOXA1 transcriptional activity analysis, 293T and other cells were transfected with SFB-tagged pcDNA3.1 vector (control) or different mutants of FOXA1, KLK3 enhancer luciferase reporter and Renilla-luc (phRL-TK, purchased from Promega, as internal control reporter). At 48 h after transfection, the renilla and firefly luciferase activities were measured with luminometry using the Dual-Luciferase Reporter Assay System (Promega) and the ratio was calculated. Results were expressed as the ratio of firefly over Renilla luciferase activity. For EMSA, The nuclear extract was from DU145 cells expressing exogenous FOXA1 and other proteins as indicated. We used sixty base pairs of forkhead response element in the *KLK3* enhancer (centered at the FOXA1 consensus binding motif 5'-GTAAACAA-3': 5'-ACATATTGTATCGATTGTCCTTGACAGTAAACAAATCTGTTGTAAGAGACATTATCTTTA-3') and the ISRE probe (5'-CTCCCCTGAGTTTCACTTCTTCTCCCAACTTG-3'). These oligoes were synthesized through the Integrated Device Technology (IDT) and labelled with biotin using Biotin 3'-End DNA labelling kit (# 89818, Thermo Fisher Scientific) and annealed to generate a labelled double stranded DNA duplex. Binding reactions were carried out in 20 µl volumes containing 2 µl of the nuclear lysates, 50 ng/µl poly(dI.dC), 1.25% glycerol, 0.025% Nonidet P-40 and 5 mM $MgCl_2$. Biotin labelled *KLK3* enhancer probe (10 fmol) was added and incubated for 1 h at room temperature, size-separated on a 6% DNA retardation gel at 100 V for 1 h in 0.5× TBE buffer, and transferred on Biodyne Nylon membrane (# 77015, Thermo Fisher Scientific) and crosslinked to the membrane using the UV light at 120 mJ/cm^2 for 2 min. Biotin-labelled free and protein-bound DNA was detected using HRP-conjugated antibody and developed using Chemiluminescent Nucleic Acid Detection Module Kit (# 89880, Thermo Fisher Scientific) according to the manufacturer's protocol.

Biotin-labeled DNA pulldown assay followed by co-IP assay

To explore the effect of FOXA1 on the DNA binding ability of STAT2 in vitro, biotin labeled-ISRE DNA was used to pull down STAT2 proteins (from chromatin-free nuclear extract treated with IFNα in FOXA1 negative DU145 cells) in the presence or absence of FOXA1 proteins

(produced by in vitro transcription/translation system). The biotin labeled-ISRE DNA was generated by biotin using Biotin 3'-End DNA labelling kit as mentioned above. The chromatin-free nuclear extract from DU145 cells with or without IFNα treatment was prepared by Subcellular Protein Fractionation Kit (Thermo Fisher Scientific, #78840) following the manufacturer's protocol. The FOXA1 and its mutant proteins were produced by TNT Quick Coupled Transcription/Translation System (Promega, # L1170) following the manufacturer's instructions. For the DNA pulldown assay, 10 pmol biotinylated DNA duplex was incubated with the nucleoplasm from DU145 (1×10^6 cells) and different dose of FOXA1 proteins in binding buffer (10 mM Tris-Cl pH7.5, 100 mM NaCl, 0.01% NP40 and 10% glycerol) overnight at 4˚C. Streptavidin-coupled sepharose beads (Cell Signaling Technology, #3419) were added the next day, and incubated for another 2 hours with the samples. The unbound supernatant was collected and anti-Flag M2 beads (Sigma-Aldrich, #A2220) were added for further Flag IP. The beads were collected and washed with binding buffer five times. The beads were subsequently boiled in 1× loading buffer and analyzed by western blotting.

Tumor cell injection and treatment

For TRAMP-C2 model, TRAMP-C2 cells (3×10^6) transfected with Vector, FOXA1-WT, FOXA1△αH3 or FOXA1△SBR were injected subcutaneously into the right flank of 8-week old male C57BL/6 (purchased from Jackson Laboratories (Bar Harbor, ME, USA)) on day 0. When the average tumor volume reached about 100 mm^3, PolyI:C (2.5 mg/kg, 100 μl) purchased from Sigma-Aldrich (# P1530) or vehicle (PBS, 100 μl) was administered by intratumoral injection every two days for two weeks and tumors were measured twice per week until the tumor volume reached the maximum allowed size. The tumor volume was calculated using a formula of length × width × width × 0.5. For CyTOF, immunofluorescence cytochemistry and RT-qPCR experiments, mice were euthanized at 48 h post the last administration of PolyI:C. The protocol for the animal experiment was approved by the Mayo Clinic Institutional Animal Cure and Use Committee (IACUC).

For MyC-CaP model, MyC-CaP cells (3×10^6) transfected doxycycline-inducible pINDUCER10-shFoxa1 (MyC-CaP$^{IN\text{-}shFoxa1\#1}$) were injected subcutaneously into the right flank of 6-week old male FVB mice (purchased from Jackson Laboratories (Bar Harbor, ME, USA)). When the average tumor volume reached about 120 mm^3, mice were randomized into groups

subsequently received 5% sucrose only (Dox-) or 5% sucrose plus 1 mg/mL doxycycline (Sigma, #D-9891) (Dox+) receptively. All water bottles were freshly prepared every second day, protected from light. Meanwhile, mice were treated with antibodies delivered using 100ul volumes and injected every four days for the following: non-specific control IgG (350 μg/dose, #BE0083, BioXcell) or combination of anti-CTLA4 (100 μg/dose, #BE0131, BioXcel) and anti-PD1 (250 μg/dose, #BE0146, BioXcel) (6) receptively. Tumors were measured with calipers and mice weighed twice a week. Mice whose tumors reached 500 mm^3 were euthanized. For Flow cytometry analysis, immunofluorescence cytochemistry and RT-qPCR experiments, mice were euthanized at 48 h post the last administration of the antibodies. The protocol for the animal experiment was approved by the Mayo Clinic Institutional Animal Cure and Use Committee (IACUC).

Flow cytometry analysis (FCA)

Tumor samples were digested to single cells with tumor dissociation kit (Miltenyi Biotec, # 130-096-730) following the manufacturer's protocol and then samples were fixed with FOXP3 Fixation/Permeabilization 1× working solution by diluting 4× Fixation/Permeabilization Concentrate (eBioscience, # 00-5123-43) with Fixation/Permeabilization Diluent (eBioscience, # 00-5223-56) at 1:4 dilution for 45 min at room temperature. Samples were stained with anti-FoxA1 (1:200 dilution; # ab23738, Abcam), Alexa Fluor 647 anti-CD8a (1:200 dilution; # 100724, BioLegend) and Alexa Fluor 594 anti-granzyme B (1:200 dilution; #ABIN6826724, Antibodies-online) and subsequently stained with secondary antibodies cross-adsorbed Alexa Fluor 488 goat anti-rabbit IgG (1:500 dilution; Invitrogen, # A-11037) for 30 min. Flow data were collected on BD FACSCanto™ flow cytometer and analyzed using FlowJo v10.

Single-cell mass cytometry (CyTOF) analysis

Single tumor cells were isolated using the mouse tumor dissociation kit (Miltenyi Biotec, # 130-096-730) following the manufacturer's protocol. CyTOF staining panels are detailed in Supplementary Table 5. The separated single cells were filtered through 40 μm filters into RPMI-1640 and centrifuged at 300 g for 5 min at 4 °C. All single cells were depleted of erythrocytes by hypotonic lysis for 1 min at room temperature. Cells were washed once with PBS and incubated with 0.5 mM of Cell-IDTM Cisplatin (Fluidigm, # 201064) for 5 min. 5 ×

10^6 or fewer cells per tumor were blocked with FcR Blocking Reagent (Miltenyl Biotec, # 130-059-901) for 10 min and incubated with surface antibody mix for 45 min at room temperature. Cells were washed with MaxPar Cell Staining Buffer (Fluidigm, # 201068).
For intracellular staining, cells were incubated with FOXP3 Fixation/Permeabilization 1× working solution by diluting 4× Fixation/Permeabilization Concentrate (eBioscience, # 00-5123-43) with Fixation/Permeabilization Diluent (eBioscience, # 00-5223-56) at 1:4 dilution for 45 min at room temperature (keep in dark). Cells were washed twice with 1× working solution of Permeabilization Buffer (eBioscience, # 00-8333-56) and centrifuged at 800g for 5min. The supernatant was carefully aspirated and the pellet was resuspend in 500 µL CyPBS diluted with 10× PBS (Rockland Immunochemicals, # MB-008) in Maxpar water (Fluidigm, # 201069). Samples were fixed with 500 µl of 2× fixation solution 4% Paraformaldehyde diluted from 16% Paraformaldehyde Aqueous Solution (Electron Microscopy Sciences, # 915710S) in CyPBS and incubated at 4°C overnight. Cells were washed with 1 ml Maxpar Cell Staining Buffer (Fluidigm; # 201068) and centifuged at 800 × g for 5 min at room temperature and resuspended in 1 ml 12.5 nM intercalation solution by diluting 125 µM intercalator stock (Cell-IDTM lntercalator-Ir- 125 µM, Fluidigm, Part No. 201192A) at 1:10,000 with Maxpar Fix and Perm Buffer-100 mL (Fluidigm; # 201067). The samples were washed with 1 ml of CyPBS and EQ beads (Fluidigm; # 201078) were added. Cells were counted on Countess II and re-suspended to approximately 5×10^5 cells/mL. Samples were filtered through 35 µm blue cap FACS tube (Falcon, #352235) and were analyzed with CyTOF instrument (Fluidigm) in the Flow Cytometry and Cellular Imaging Core Facility at Mayo Clinic. Data were analyzed with PhenoGraph by following the instruction (7). R studio (Version 1.0.136) was downloaded from the official R website (www.r-project.org/). The cytofkit package (Release 3.6) was downloaded from Bioconductor (https://www.bioconductor.org/packages/release/bioc/html/cytofkit.html) and opened in R. The gated singlet (19Ir + 193Ir +), viable (195Pt +) events were imported into cytofkit, subjected to PhenoGraph analysis, and clustered on the basis of markers. The files were clustered with the PhenoGraph algorithm and tSNE was selected as the visualization method. 44 unique clusters were identified using PhenoGraph. The unique clusters identified with PhenoGraph were visualized via the R package “Shiny,” where labels, dot size, and cluster color were customized. Clusters were colored according to the phenotype based on the median expression of various markers. The frequency of each cluster was determined via csv files generated by the algorithm.

The Percentage of each cell population was analyzed with the FlowJo and GraphPad Prism 8 software.

Immunofluorescence cytochemistry

Formalin-fixed paraffin-embedded TRAMP-C2 and MyC-CaP tumor samples were deparaffinized, rehydrated and subjected to heat-mediated antigen retrieval. Sections were incubated with 1% Sudan Black (dissolved in 70% ethanol) for 20 min at room temperature to reduce autofluorescence. Slides were washed with 0.02% Tween 20 and incubated with 0.1 M Glycine for 10 min. And immersed slides in 10 mg/ml Sodium Borohydride in ice cold Hanks Buffer on ice for 40 mins. After washing with two times PBS, slides were blocked by 1% BSA in PBS for 30 mins and incubated with FOXA1 antibody (1:1000 dilution; Abcam, # ab170933) and anti-mouse CD8 (1:1000 dilution; Santa Cruz Biotechnology, #sc-1177) at 4°C overnight. The sections were washed three times in 1× PBS and treated with secondary antibodies cross-adsorbed Alexa Fluor 594 goat anti-rabbit IgG (1:500 dilution; Invitrogen, # A-11037) or cross-adsorbed Alexa Fluor 488 goat anti-mouse IgG (1:500 dilution; Invitrogen, # A11001) for 30 min. Prior to imaging, sample were mounted with VECTASHIELD Antifade Mounting Medium with DAPI (Fisher Scientific, #NC9524612). Samples were imaged using Nikon spinning disk confocal.

Tumor mutational burden (TMB) analysis

TMB was calculated according to previously defined methods (8, 9). We calculated TMB using exome data, including only non-silent mutations, as defined below. We only consider as somatic mutations: Frameshift Deletions, Frameshift Insertons, In-Frame Deletions, In-Frame Insertions, Missense Mutations, Nonsense Mutations, Nonstop Mutations, Splice Sites, Translation Start Sites and we ignore the following silent variants: 3'Flanks, 3'UTRs, 5'Flanks, 5'UTRs, IGRs, Introns, RNAs and Splice Regions. We quoted standard human exome length as 38Mb. The base substitutions and indels in the coding region of targeted genes, including synonymous mutations, were filtered for both oncogenic driver events according to COSMIC (Catalogue of Somatic Mutations in Cancer) and germline status according to dbSNP (The Single Nucleotide Polymorphism Database) and ExAC (The Exome Aggregation Consortium) databases.

Analysis of *FOXA1* mRNA expression, IFN activity and immune cell markers in prostate, breast and bladder cancers of patients treated with immunotherapy or chemotherapy

To evaluate the mRNA expression level of *FOXA1*, *CD3E*, *CD8A* and *GZMB* as well as IFN activity in patients with pathological complete response (pCR with residual cancer burden (RCB) 0 or I) and no pathological complete response (No-pCR with RCB II or III) to neoadjuvant chemotherapy (NAC) in breast cancer, RNA-seq data from Breast Cancer Genome-Guided Therapy (BEAUTY) (10) project at Mayo Clinic was analyzed. To further validate the data from the Mayo Clinic cohort, RNA-microarray data from NAC-treated breast cancer from independent cohorts (GSE106977; GSE41998; GSE34138; GSE21974) (11-14) were also analyzed similarly. To evaluate the impact of Foxa1 on immunotherapy response, IFN activity and cytotoxic T cell activities in murine breast cancer, the mRNA expression level of *Foxa1*, *CD3e*, *CD8a* and *Gzmb* as well as IFN activity from RNA-seq data (GSE124821) (15) was analyzed according to the responsiveness to anti-PD1 and anti-CTLA-4 combination therapy (resistant versus sensitive). To evaluate the impact of FOXA1 on the clinical outcome, IFN activity and cytotoxic T cell activities in metastatic castration-resistant prostate cancer (CRPC) patients treated with personalized peptide vaccination (PPV) (16), the mRNA expression level of *FOXA1*, *CD3E*, *CD8A* and *GZMB* as well as IFN activity from RNA microarray data (GSE53922) and clinical outcome was analyzed according to the *FOXA1* expression level. Similarly, we also evaluated the correlations between *FOXA1* and the clinical outcome, IFN activity as well as cytotoxic T cell activities in bladder cancers from different cohorts which treated with Bacillus Calmette-Guerin (BCG) immunotherapy (GSE19423) (17) or MVAC (methotrexate, vinblastine, doxorubicin, and cisplatin) chemotherapy (GSE70691) (18).

Clinical data and patient information of urothelial carcinomas treated with immunotherapy

Tumor samples and medical records from a cohort of 23 patients (20 males and 3 females; Age from 44 to 77 years; Median age 65 years) with urothelial carcinoma (cancers in bladder, renal pelvis, ureter or urethra that showed predominantly transitional-cell features on histologic testing) treated at Fudan University Shanghai Cancer Center were analyzed. The protocol of this study was approved by the Ethical and Scientific Committee (equivalent to Institutional Review Board (IRB)) at Fudan University Shanghai Cancer Center. Urothelial carcinoma samples were

obtained from the primary or metastatic lesions of 23 patients before they underwent therapy with anti-PD1 treatment until disease progression according to the Response Evaluation Criteria in Solid Tumors (RECIST) version 1.1,15 (19). All patients provided written consent before enrolling in the study. Formalin-fixed paraffin-embedded (FFPE) tumor specimens with sufficient viable tumor content were required before the start of the study. One sample (patient 7) was excluded for immunohistochemistry (IHC) staining evaluation because the specimen was too small. A total of 22 specimens were used for FOXA1 IHC staining evaluation.

Immunohistochemistry (IHC) of urothelial carcinoma patient specimens

Urothelial carcinoma FFPE samples were deparaffinized, rehydrated and subjected to heat-mediated antigen retrieval. Sections were incubated with 3% H_2O_2 for 15 min at room temperature to quench endogenous peroxidase activity. After antigen retrieval using unmasking solution (Vector Labs), slides were blocked with normal goat serum for 1 h and incubated with primary antibody at 4°C overnight. IHC analysis of tumor samples were performed using primary antibodies for FOXA1 (dilution 1:500; Abcam, # ab170933). The sections were washed three times in 1× PBS and treated for 30 min with biotinylated goat-anti-rabbit IgG secondary antibodies (#BA-9200, Vector Labs). After washing three times in 1× PBS, the sections were incubated with streptavidin-conjugated HRP (#3999S, Cell Signaling Technology). After washing three times in 1× PBS for 5 min each, specific detection was developed with 3,3′3diaminobenzidine (#D4168-50SET, Sigma-Aldrich). For IHC staining score (IS) or intensity, 0 = <1% positive cells, 1 = 1-20% positive cells, 2 = 20-50% positive cells, 3 = >50% positive cells. FOXA1 expression levels with IS = 0 or 1 are considered as “low” and IS = 2 or 3 are considered as “high”.

Data availability

All data and softwares used in this study are accessible. The raw data of single cell RNA-seq from prostate cancer patient tissues reported in this paper is accessible with Gene Expression Omnibus (GEO) accession number GSE141445: https://www.ncbi.nlm.nih.gov/geo/query/acc.cgi?acc=GSE141445, token: yhmhquokxjqfzgj.

The GEO accession number for the ChIP-seq and RNA-seq data from cell lines reported in this paper is GSE142221: https://www.ncbi.nlm.nih.gov/geo/query/acc.cgi?acc=GSE142221; Secure token: yderayksdtazlsr. Previously deposited transcriptomic data (GSE106977; GSE41998; GSE34138; GSE21974; GSE53922; GSE19423; GSE70691; GSE130408; GSE124821; GSE128421) that are used in this study are also available at GEO (https://www.ncbi.nlm.nih.gov/geo/).

Supplementary references

1. Robinson MD, McCarthy DJ, and Smyth GK. edgeR: a Bioconductor package for differential expression analysis of digital gene expression data. *Bioinformatics.* 2010;26(1):139-40.
2. Subramanian A, Tamayo P, Mootha VK, Mukherjee S, Ebert BL, Gillette MA, et al. Gene set enrichment analysis: a knowledge-based approach for interpreting genome-wide expression profiles. *Proc Natl Acad Sci U S A.* 2005;102(43):15545-50.
3. Mootha VK, Lindgren CM, Eriksson KF, Subramanian A, Sihag S, Lehar J, et al. PGC-1alpha-responsive genes involved in oxidative phosphorylation are coordinately downregulated in human diabetes. *Nat Genet.* 2003;34(3):267-73.
4. Zuo D, Shogren KL, Zang J, Jewison DE, Waletzki BE, Miller AL, 2nd, et al. Inhibition of STAT3 blocks protein synthesis and tumor metastasis in osteosarcoma cells. *J Exp Clin Cancer Res.* 2018;37(1):244.
5. Meerbrey KL, Hu G, Kessler JD, Roarty K, Li MZ, Fang JE, et al. The pINDUCER lentiviral toolkit for inducible RNA interference in vitro and in vivo. *Proc Natl Acad Sci U S A.* 2011;108(9):3665-70.
6. Jayaprakash P, Ai M, Liu A, Budhani P, Bartkowiak T, Sheng J, et al. Targeted hypoxia reduction restores T cell infiltration and sensitizes prostate cancer to immunotherapy. *J Clin Invest.* 2018;128(11):5137-49.
7. Kimball AK, Oko LM, Bullock BL, Nemenoff RA, van Dyk LF, and Clambey ET. A Beginner's Guide to Analyzing and Visualizing Mass Cytometry Data. *J Immunol.* 2018;200(1):3-22.
8. Chalmers ZR, Connelly CF, Fabrizio D, Gay L, Ali SM, Ennis R, et al. Analysis of 100,000 human cancer genomes reveals the landscape of tumor mutational burden. *Genome Med.* 2017;9(1):34.
9. Hellmann MD, Ciuleanu TE, Pluzanski A, Lee JS, Otterson GA, Audigier-Valette C, et al. Nivolumab plus Ipilimumab in Lung Cancer with a High Tumor Mutational Burden. *N Engl J Med.* 2018;378(22):2093-104.
10. Goetz MP, Kalari KR, Suman VJ, Moyer AM, Yu J, Visscher DW, et al. Tumor Sequencing and Patient-Derived Xenografts in the Neoadjuvant Treatment of Breast Cancer. *J Natl Cancer Inst.* 2017;109(7).
11. Horak CE, Pusztai L, Xing G, Trifan OC, Saura C, Tseng LM, et al. Biomarker analysis of neoadjuvant doxorubicin/cyclophosphamide followed by ixabepilone or Paclitaxel in early-stage breast cancer. *Clin Cancer Res.* 2013;19(6):1587-95.

12. de Ronde JJ, Lips EH, Mulder L, Vincent AD, Wesseling J, Nieuwland M, et al. SERPINA6, BEX1, AGTR1, SLC26A3, and LAPTM4B are markers of resistance to neoadjuvant chemotherapy in HER2-negative breast cancer. *Breast Cancer Res Treat.* 2013;137(1):213-23.
13. Santonja A, Sanchez-Munoz A, Lluch A, Chica-Parrado MR, Albanell J, Chacon JI, et al. Triple negative breast cancer subtypes and pathologic complete response rate to neoadjuvant chemotherapy. *Oncotarget.* 2018;9(41):26406-16.
14. Stickeler E, Pils D, Klar M, Orlowsk-Volk M, Zur Hausen A, Jager M, et al. Basal-like molecular subtype and HER4 up-regulation and response to neoadjuvant chemotherapy in breast cancer. *Oncol Rep.* 2011;26(4):1037-45.
15. Hollern DP, Xu N, Thennavan A, Glodowski C, Garcia-Recio S, Mott KR, et al. B Cells and T Follicular Helper Cells Mediate Response to Checkpoint Inhibitors in High Mutation Burden Mouse Models of Breast Cancer. *Cell.* 2019;179(5):1191-206 e21.
16. Araki H, Pang X, Komatsu N, Soejima M, Miyata N, Takaki M, et al. Haptoglobin promoter polymorphism rs5472 as a prognostic biomarker for peptide vaccine efficacy in castration-resistant prostate cancer patients. *Cancer Immunol Immunother.* 2015;64(12):1565-73.
17. Kim YJ, Ha YS, Kim SK, Yoon HY, Lym MS, Kim MJ, et al. Gene signatures for the prediction of response to Bacillus Calmette-Guerin immunotherapy in primary pT1 bladder cancers. *Clin Cancer Res.* 2010;16(7):2131-7.
18. McConkey DJ, Choi W, Shen Y, Lee IL, Porten S, Matin SF, et al. A Prognostic Gene Expression Signature in the Molecular Classification of Chemotherapy-naive Urothelial Cancer is Predictive of Clinical Outcomes from Neoadjuvant Chemotherapy: A Phase 2 Trial of Dose-dense Methotrexate, Vinblastine, Doxorubicin, and Cisplatin with Bevacizumab in Urothelial Cancer. *Eur Urol.* 2016;69(5):855-62.
19. Eisenhauer EA, Therasse P, Bogaerts J, Schwartz LH, Sargent D, Ford R, et al. New response evaluation criteria in solid tumours: revised RECIST guideline (version 1.1). *Eur J Cancer.* 2009;45(2):228-47.

Supplementary Figure 1

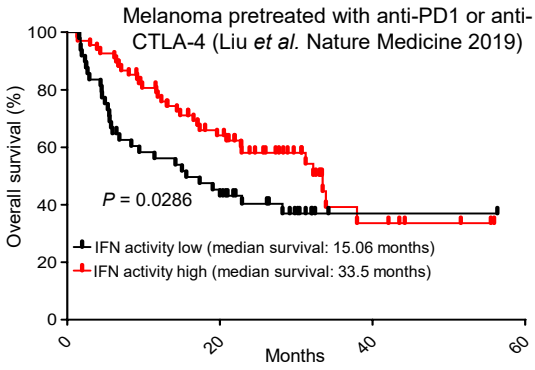

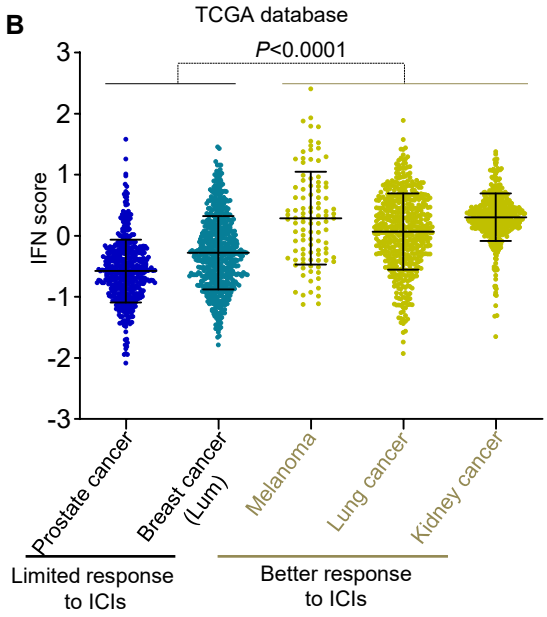

C

Spearman rank of top genes negatively coefficient with IFN activity

Prostate cancer (TCGA)

Genes	Spearman's rho	P-value
ACACA	-0.56348	1.74E-42
FOXA1	-0.53136	3.99E-37
C9ORF152	-0.53029	5.88E-37
RAB3IP	-0.52284	8.48E-36
SLC35E1	-0.52243	9.82E-36
LEO1	-0.51939	2.85E-35
MAML3	-0.51089	5.35E-34
ERGIC1	-0.50862	1.16E-33
GALNT7	-0.50333	6.78E-33
PPM1H	-0.50109	1.42E-32
ACLY	-0.4919	2.80E-31
SHANK2	-0.49052	4.34E-31
PPP1R9A	-0.48824	8.92E-31
TTC3	-0.48706	1.29E-30
CMTM4	-0.48546	2.14E-30
TMEM268	-0.48425	3.12E-30
KCTD3	-0.48253	5.32E-30
LRIG1	-0.47984	1.22E-29
DOP1B	-0.47958	1.32E-29
BEND4	-0.47624	3.65E-29
SCARB2	-0.47571	4.29E-29
TMEM192	-0.47546	4.63E-29
ZNF24	-0.47532	4.82E-29
GSE1	-0.47468	5.86E-29
TOM1L1	-0.47382	7.59E-29
GFPT1	-0.47254	1.12E-28
HIPK2	-0.47152	1.51E-28
REPS2	-0.47125	1.64E-28
MBOAT2	-0.47096	1.79E-28
DSC2	-0.46895	3.25E-28
IQGAP2	-0.46689	5.96E-28
GOLPH3	-0.46675	6.22E-28
UAP1	-0.46672	6.28E-28
TAB3	-0.46669	6.33E-28
GNPNAT1	-0.46557	8.80E-28
MMUT	-0.46547	9.06E-28
FNBP1L	-0.46511	1.01E-27
ZBED4	-0.46376	1.49E-27
LARS	-0.4633	1.70E-27
ZNF542P	-0.46278	1.98E-27
SLC46A1	-0.46071	3.61E-27
SMARCC1	-0.46065	3.67E-27
TMTC4	-0.45951	5.09E-27
PLA2G12A	-0.45926	5.47E-27
VPS54	-0.45911	5.72E-27
STEAP2	-0.45624	1.29E-26
CANT1	-0.45598	1.40E-26
PHKB	-0.45593	1.41E-26
NWD1	-0.45575	1.49E-26

Breast cancer (TCGA)

Genes	Spearman's rho	P-value
TOM1L2	-0.38571	1.31E-36
SUMF1	-0.37199	5.59E-34
FAM172A	-0.36778	3.38E-33
XBP1	-0.35779	2.19E-31
FOXA1	-0.35233	2.00E-30
CASZ1	-0.3465	2.03E-29
EIF4B	-0.34103	1.71E-28
KDM4B	-0.33776	6.01E-28
FAM47E	-0.33671	8.95E-28
MTURN	-0.33189	5.50E-27
THSD4	-0.33164	6.04E-27
NEDD4L	-0.33157	6.20E-27
KIAA1324	-0.33145	6.49E-27
BCAM	-0.33137	6.66E-27
KIAA0556	-0.3294	1.39E-26
PLA2G12A	-0.32827	2.10E-26
EEF2	-0.32789	2.41E-26
CYB5D2	-0.32748	2.80E-26
ZNF396	-0.32673	3.69E-26
HCAR1	-0.32657	3.92E-26
ERBB3	-0.32586	5.08E-26
USP22	-0.32474	7.63E-26
RUNDC1	-0.32359	1.16E-25
MLPH	-0.32198	2.07E-25
KIF13B	-0.32186	2.16E-25
ZBTB42	-0.32076	3.20E-25
ALDH6A1	-0.31868	6.72E-25
DRC3	-0.31866	6.77E-25
UNC119B	-0.31678	1.32E-24
ARSD	-0.31668	1.36E-24
SPRED2	-0.31587	1.81E-24
ERBB4	-0.31474	2.70E-24
LONRF2	-0.31446	2.97E-24
LMX1B	-0.3141	3.37E-24
GLUD1	-0.31332	4.42E-24
IFT140	-0.31273	5.42E-24
REEP6	-0.31113	9.45E-24
RERE	-0.30985	1.47E-23
MEGF9	-0.30974	1.53E-23
PCDH1	-0.30938	1.72E-23
MOAP1	-0.30871	2.17E-23
ARSG	-0.30825	2.53E-23
MAPT	-0.308	2.76E-23
POLI	-0.30773	3.03E-23
CACNA1D	-0.30764	3.12E-23
ATP8B1	-0.30749	3.29E-23
SHROOM3	-0.30686	4.07E-23
THRB	-0.30637	4.80E-23
IGF1R	-0.30451	8.98E-23

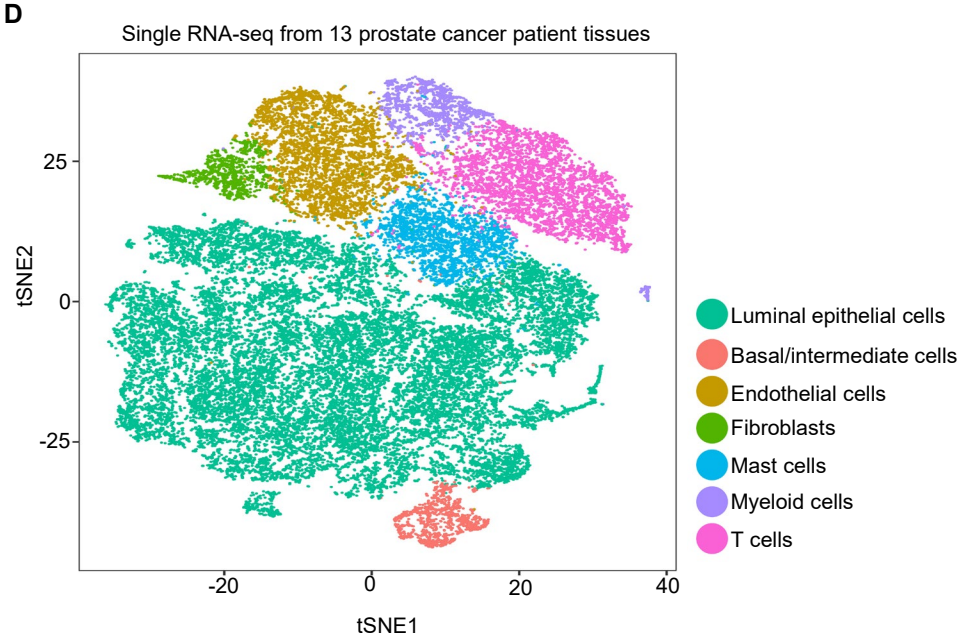

Supplementary Figure 1. Inverse correlation between *FOXA1* mRNA expression and IFN signaling and APM genes in prostate and breast cancer patient samples. (Related to Figure 1)

A. Overall survival of patients with IFN activity-low or -high in the cohort of melanoma pretreated with anti-PD1 or anti-CTLA-4 (Liu *et al.* Nature Medicine 2019). Statistical significance was determined by Log-rank (Mantel-Cox) test (n = 117). (See details in Methods for the calculation of IFN gene expression score.)

B. Comparison of IFN score in prostate cancer and luminal breast cancer with melanoma, lung and kidney cancers from TCGA database. Data shown as means ± SD; Statistical significance was determined by one-way analysis of variance (ANOVA).

C. Spearman rank of top genes negatively correlated to IFN score in the TCGA cohorts of prostate and breast cancers. Statistical significance was determined by Spearman's rho correlation test.

D. T-SNE projections of ten stages from single cell RNA sequencing data. T-SNE plot was performed for the entire dataset (n = 53,090 cells) and cells are colored and labelled by clusters. The luminal epithelial cells (n = 23,674) were used for the heatmap shown in Figure 1B. Clinic information of patients is shown in Supplementary Table 1 and Supplementary Table 2.

Supplementary Figure 2

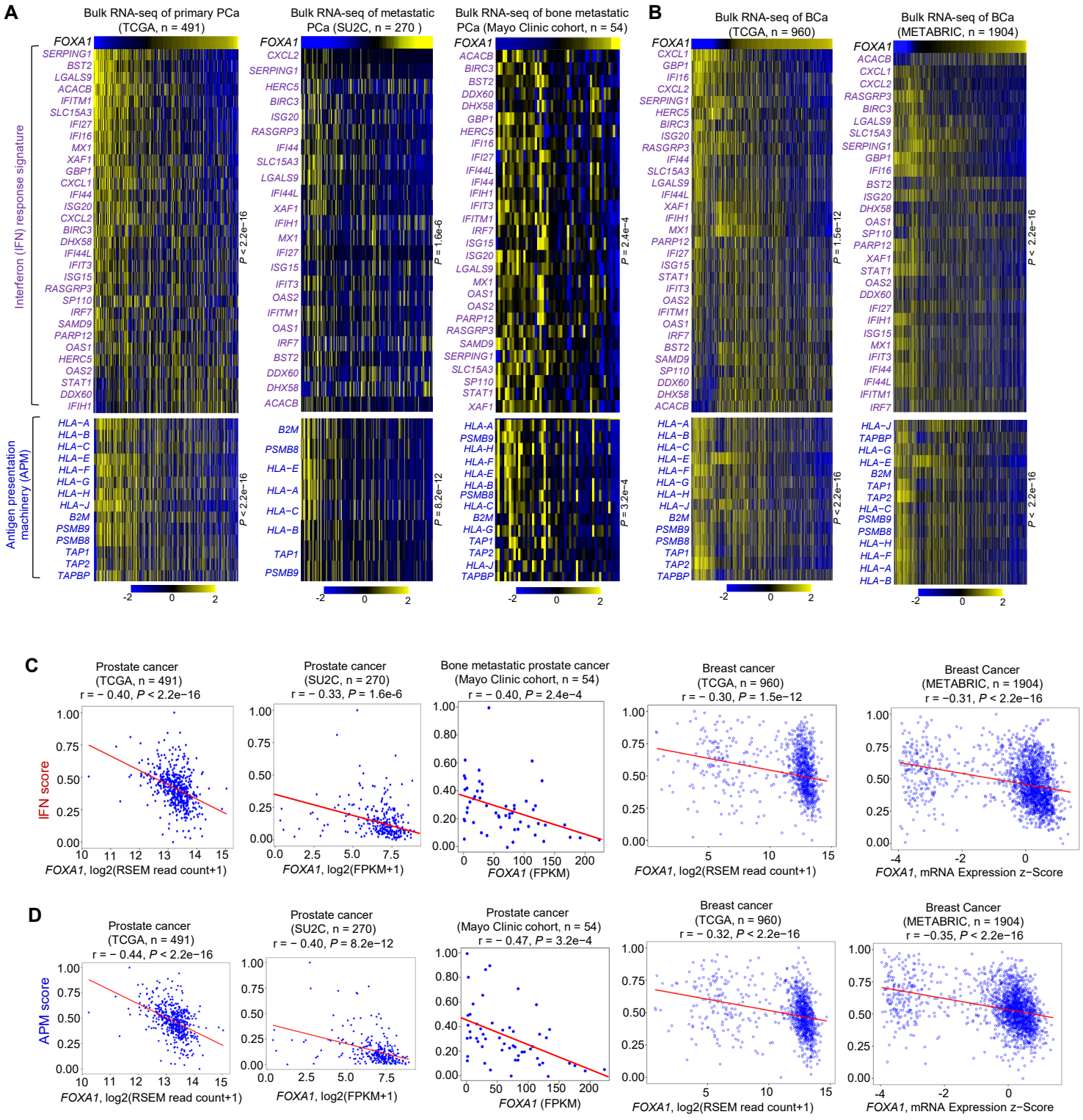

Supplementary Figure 2. Inverse correlation between *FOXA1* mRNA expression and IFN signaling and APM genes in prostate and breast cancer patient samples. (Related to Figure 1)

A. Heatmaps show the inverse correlation of *FOXA1* expression with IFN response signature genes and APM genes in bulk tissue RNA-seq data of PCa samples. Statistical significance was determined by Pearson correlation test.

B. Heatmaps show the inverse correlation of *FOXA1* expression with IFN response signature genes and APM genes in bulk tissue RNA-seq data of BCa samples. Statistical significance was determined by Pearson correlation test.

C. The correlation of *FOXA1* level with IFN score (see details in Methods for the calculation of gene expression score) in TCGA, SU2C, Mayo Clinic cohorts of prostate cancer and TCGA and METABRIC cohorts of breast cancer. Statistical significance was determined by Pearson correlation test.

D. The correlation of *FOXA1* level with APM score (see details in Methods for the calculation of gene expression score) in TCGA, SU2C, Mayo Clinic cohorts of prostate cancer and TCGA and METABRIC cohorts of breast cancer. Statistical significance was determined by Pearson correlation test.

Supplementary Figure 3

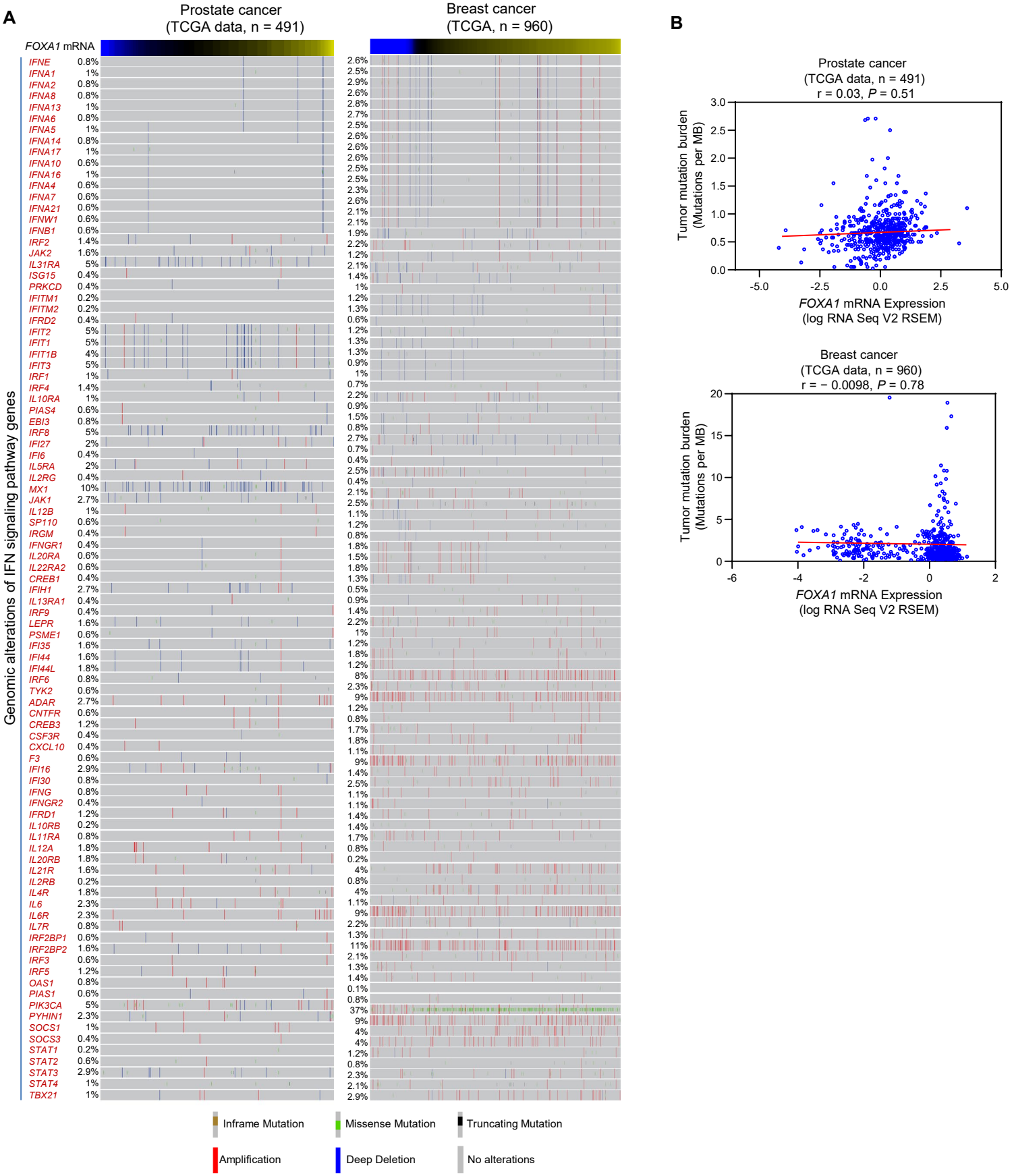

Supplementary Figure 3. *FOXA1* expression is not associated with genomic alterations in IFN signaling pathway genes and tumor mutation burden (TMB). (Related to Figure 1)

A. Heatmaps show that there was no obvious correlation between *FOXA1* expression and the genomic alterations in the IFN signaling pathway genes in the TCGA cohorts of prostate and breast cancer. Samples are ranked based on *FOXA1* transcript levels.

B. The correlation between *FOXA1* level and TMB in TCGA cohorts of prostate cancer and breast cancer. Statistical significance was determined by Pearson correlation test.

Supplementary Figure 4

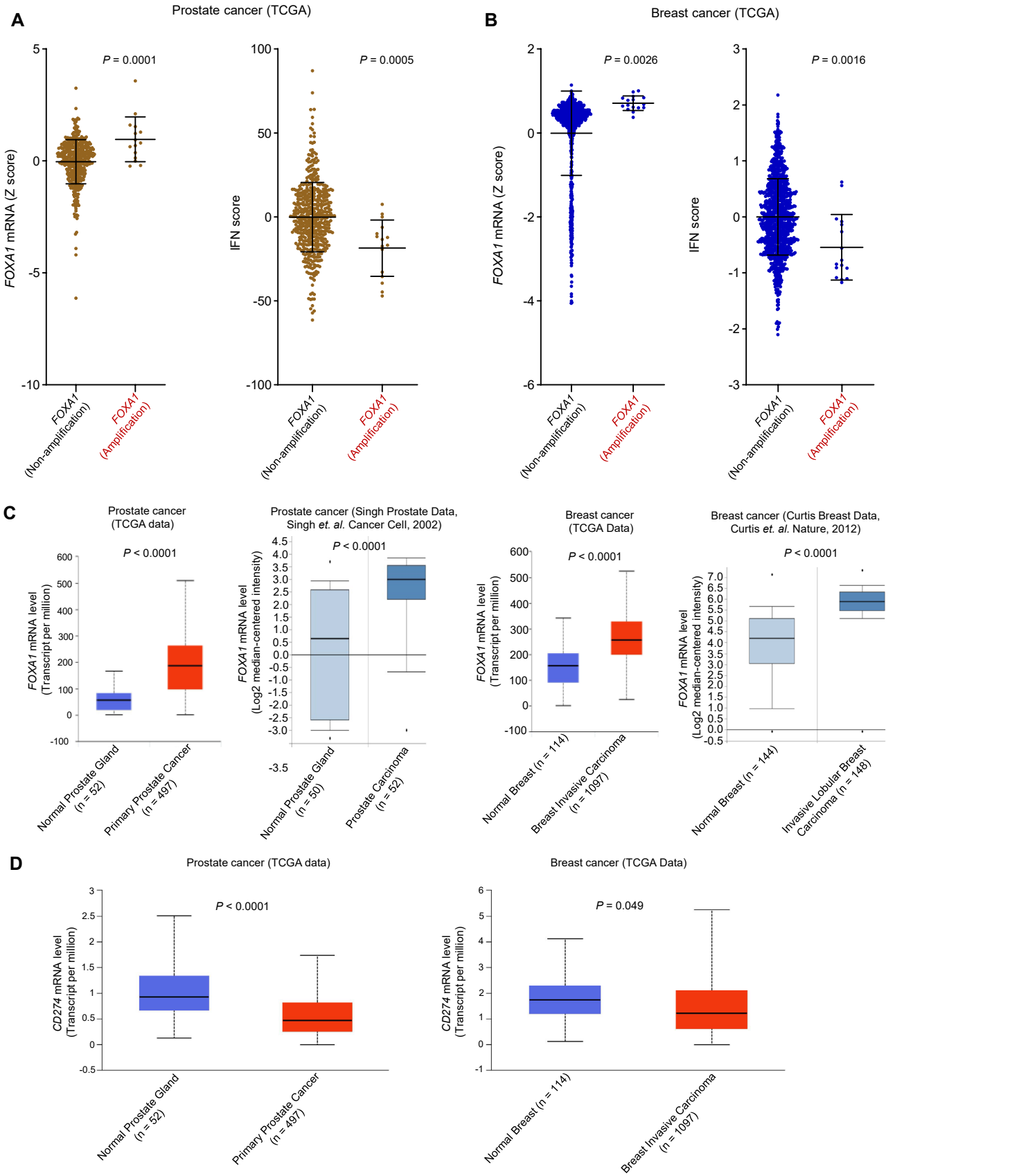

Supplementary Figure 4. *FOXA1* mRNA is overexpressed and *CD274* mRNA is downregulated in prostate and breast cancer patients. (Related to Figure 1)

A. Relative *FOXA1* mRNA level and IFN score in the cases of *FOXA1* amplification and non-amplification in prostate cancer from cohorts of TCGA. Data shown as means ± SD; Statistical comparison was done using Mann-Whitney U test.

B. Relative *FOXA1* mRNA level and IFN score in the cases of *FOXA1* amplification and non-amplification in breast cancer from cohorts of TCGA. Data shown as means ± SD; Statistical comparison was done using Mann-Whitney U test.

C. Comparison of *FOXA1* mRNA level between normal tissues and tumor tissues in the indicated cohorts of prostate or breast cancer. Data shown as means ± SD; Statistical comparison was done using Mann-Whitney U test.

D. Comparison of *CD274* (PD-L1) mRNA level between cancer specimens and normal tissues in the TCGA cohorts of prostate or breast cancers. Data shown as means ± SD; Statistical comparison was done using Mann-Whitney U test.

Supplementary Figure 5

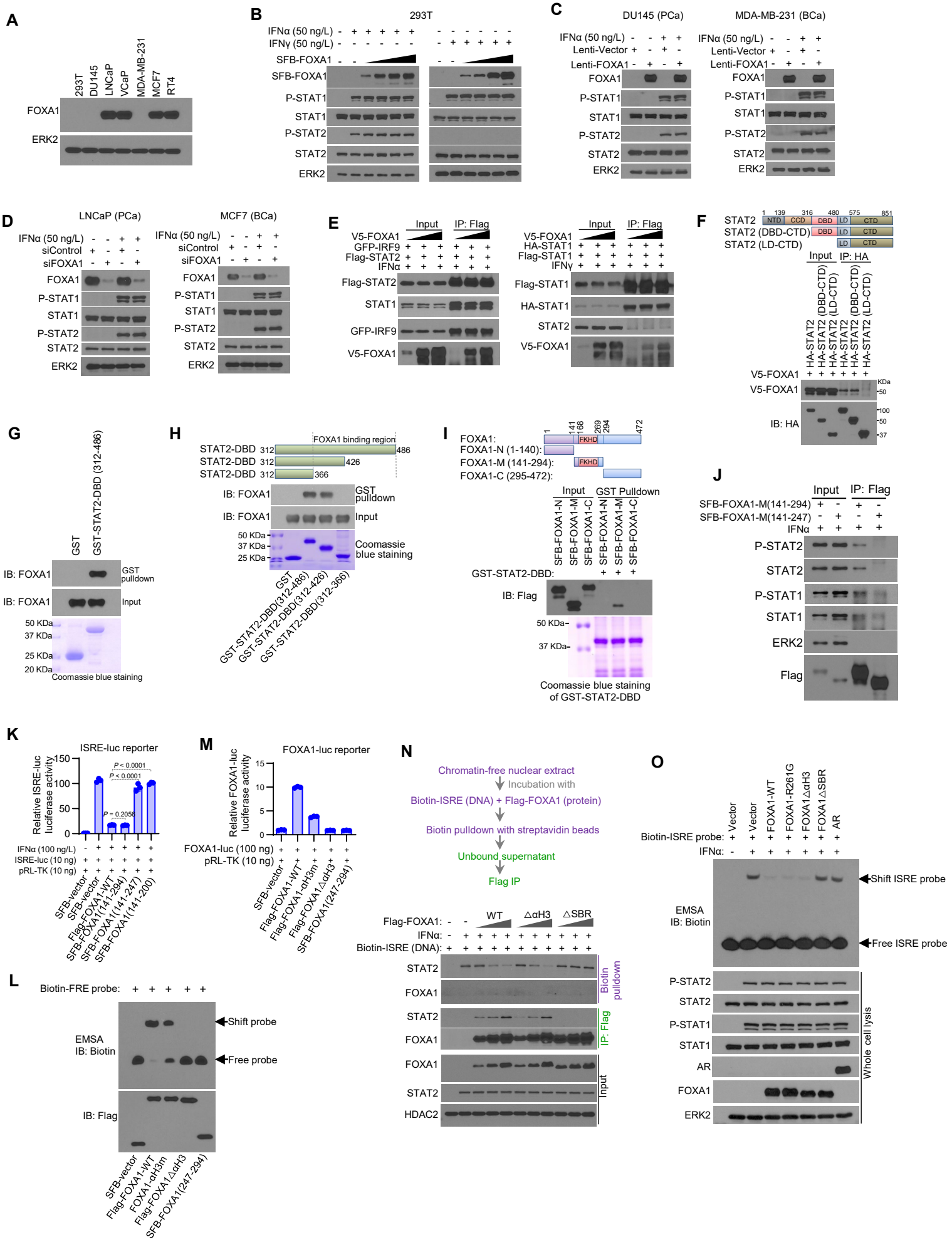

Supplementary Figure 5. Effects of FOXA1 on expression of total and phosphorylated STAT1 and STAT2 proteins and STAT2 activity. (Related to Figure 2)

A. Western blot analysis of expression of FOXA1 protein in the indicated cell lines. ERK2 was used as a loading control.

B. Western blot analysis of the indicated proteins in 293T cells transfected with SFB-tagged FOXA1 in different doses in the presence or absence of IFNα or IFNγ.

C. Western blot analysis of the indicated proteins in FOXA1-negative DU145 PCa and MDA-MB-231 BCa cells infected with lentivirus expressing vector or FOXA1 and treated with or without IFNα.

D. Western blot analysis of the indicated proteins in FOXA1-high LNCaP PCa or MCF7 BCa cells transfected with control or FOXA1-specific siRNAs and treated with or without IFNα.

E. Co-IP analysis of the effect of FOXA1 on the formation of STAT1-STAT2-IRF9 and STAT1-STAT1 complexes in 293T cells.

F. Co-IP analysis of interaction of FOXA1 with STAT2 full length or its N-terminal truncation mutants in 293T cells. NTD, N-terminal domain; CCD, coiled-coil domain; DBD, DNA binding domain; LD, linker domain; CTD, C-terminal domain.

G. GST pulldown examining the interaction of FOXA1 with STAT2 DBD in vitro. STAT2 DBD protein was purified from *E.coli* and FOXA1 protein was produced by in vitro transcription/translation.

H. GST pulldown analysis of the interaction of GST-tagged STAT2 DBD and its C-terminal truncation mutants with FOXA1 protein produced by in vitro transcription/translation.

I. GST pulldown analysis of the interaction of GST-tagged STAT2 DBD with different fragments of FOXA1 protein produced by in vitro transcription/translation. FKHD, forkhead domain; N, N-terminal; M, middle portion; C, C-terminal.

J. Co-IP analysis of the interaction of SFB-tagged FOXA1 truncation mutants FOXA1(141-294) and FOXA1(141-247) with STAT1 and STAT2 in 293T cells treated with IFNα.

K. Luciferase reporter assay performed to assess the effect of FOXA1 WT and truncation mutants on IFN stimulation response element luciferase reporter (ISRE-luc) activity in 293T cells treated with IFNα. Data shown as means ± SD (n = 3); Statistical significance was determined by one-way ANOVA with Bonferroni correction for multiple tests.

L. EMSA assay performed to analyze the binding of FOXA1 WT and indicated mutants to the FOXA1 response element (FRE) present in the *KLK3* (PSA) gene enhancer.

M. Luciferase reporter assay performed to determine the effect of FOXA1 WT and indicated mutants on the activity of luciferase reporter containing FOXA1 response element (FRE) derived from the *KLK3* gene enhancer in 293T cells. Data shown as means ± SD (n = 3).

N. Biotin-labeled DNA pulldown assay followed by co-IP assay (see Supplementary Methods). ISRE, interferon stimulation response element.

O. EMSA assay. Biotin-labeled ISRE was incubated with nuclear extract of vehicle- or IFNα-treated DU145 cells expressing FOXA1 WT, FOAX1 mutants or AR prior to PAGE and/or Western blots.

Supplementary Figure 6

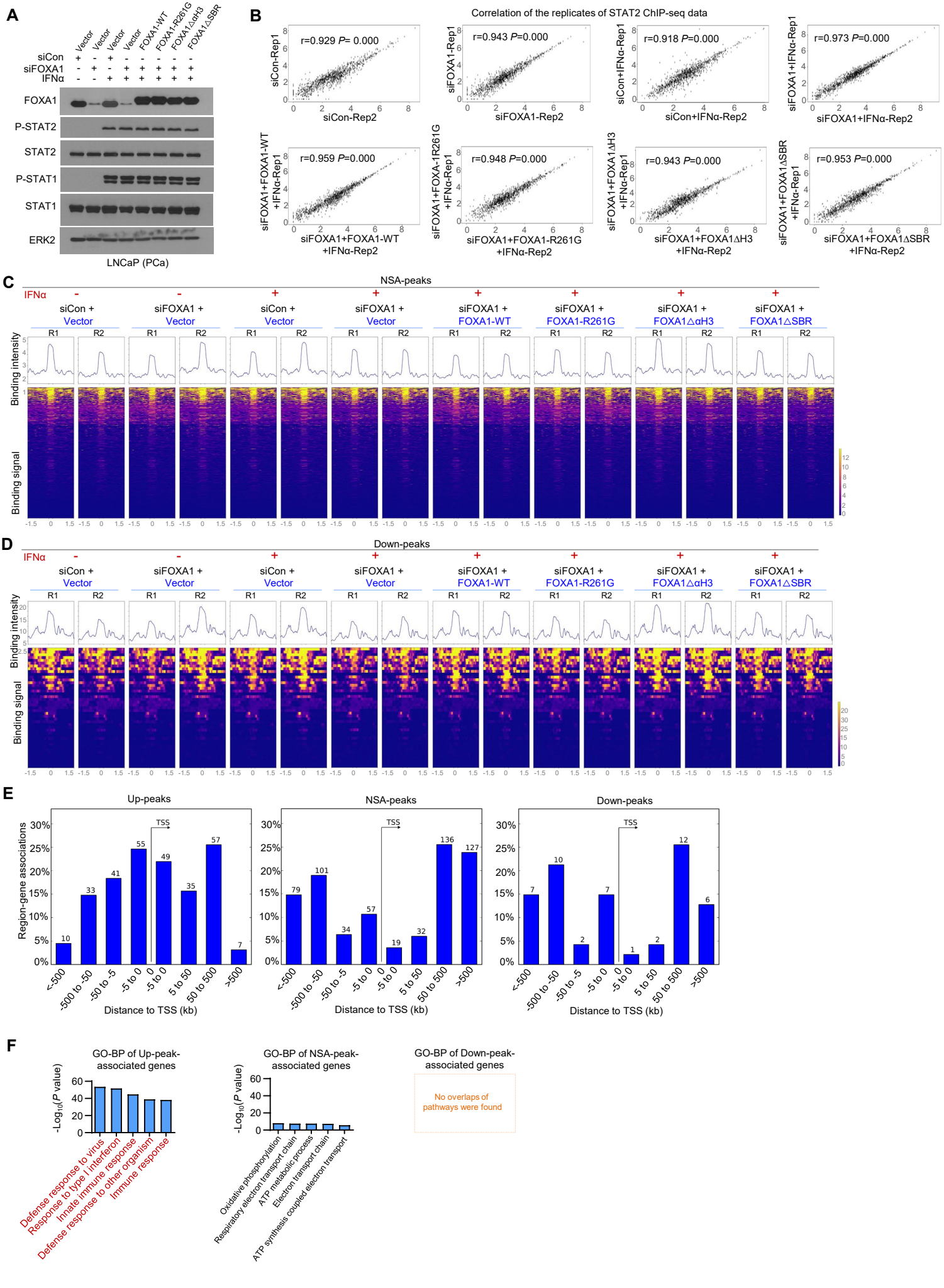

Supplementary Figure 6. Effect of FOXA1 expression on STAT2 occupancy on chromatin in LNCaP cells. (Related to Figure 3)

A. Western blot analysis of indicated proteins in indicated LNCaP cells. LNCaP cells stably expressing vector, FOXA1 WT or mutants were transfected with control (siCon) or FOXA1-specific siRNA (siFOXA1) followed by treatment with vehicle or IFNα. Independent sets of cells were also used for STAT2 ChIP-seq.
B. Analysis of correlation between replicates of STAT2 ChIP-seq data in each indicated cellular condition.
C. The STAT2 binding intensity (top) and binding signal heatmap (bottom) of NSA-peaks (identified by STAT2 ChIP-seq as shown in Figure 3A) in the indicated cellular conditions.
D. The STAT2 binding intensity (top) and binding signal heatmap (bottom) of Down-peaks (identified by STAT2 ChIP-seq as shown in Figure 3A) in the indicated cellular conditions.
E. Distributions of STAT2 ChIP-seq peaks (Up, NSA or Down) in the genome relative to the transcription start site (TSS).
F. GO-BP pathways analysis of genes associated with STAT2 ChIP-seq Up-peaks, NSA-peaks and Down-peaks.

Supplementary Figure 7

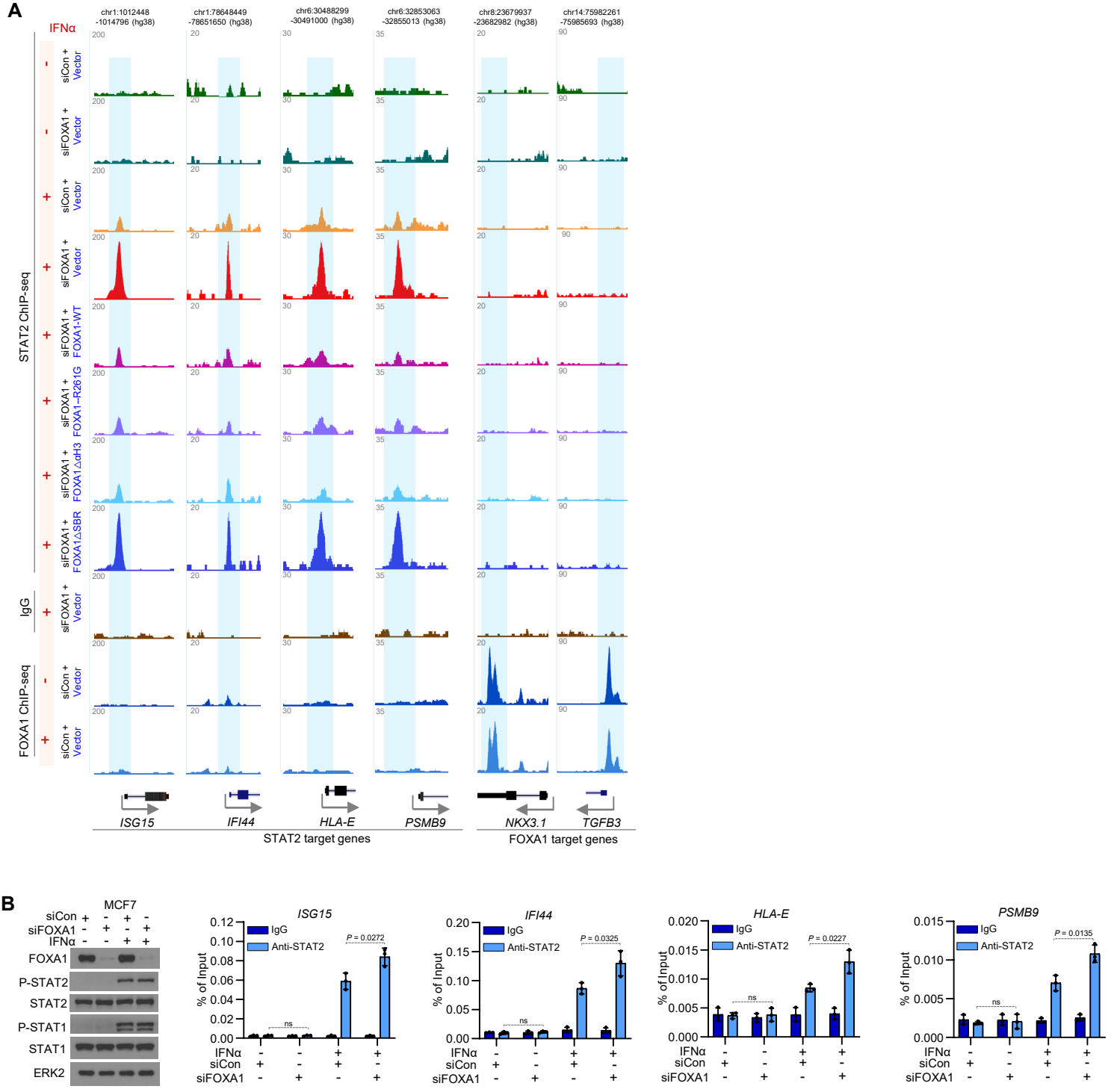

Supplementary Figure 7. Effect of FOXA1 expression on STAT2 occupancy on chromatin in LNCaP cells. (Related to Figure 3)

A. UCSC tracks (integration of two replicates) show ChIP-seq signals of IgG, STAT2 and FOXA1 at genomic loci of STAT2 target genes *ISG15*, *IFI44*, *HLA-E*, *PSMB9* and of FOXA1 target genes *NKX3.1* and *TGFB3*.

B. STAT2 ChIP-qPCR validation of STAT2 occupancy at genomic loci of Stat2 target genes *ISG15*, *IFI44*, *HLA-E* and *PSMB9* in MCF7 cells transfected with control (siCon) or FOXA1-specific siRNAs (siFOXA1) and treated with or without IFNα. Data shown as means ± SD (n = 3). Statistical significance was determined by one-way ANOVA with Bonferroni correction for multiple tests.

Supplementary Figure 8

A

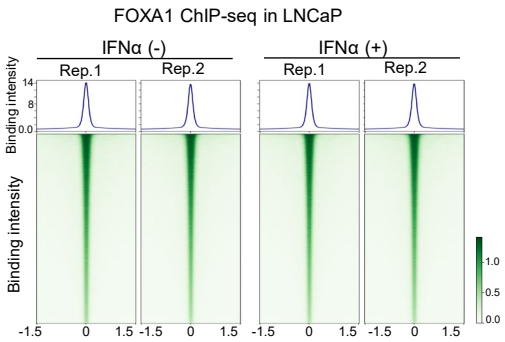

B

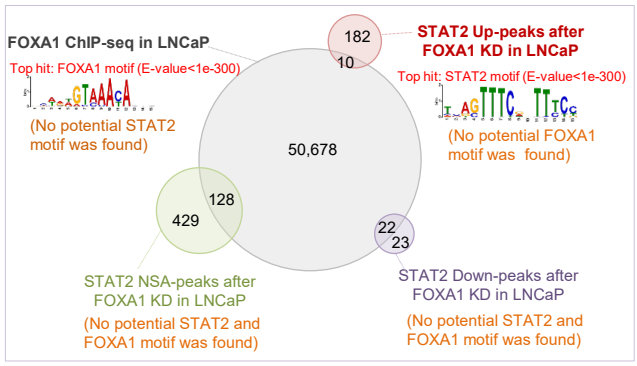

C

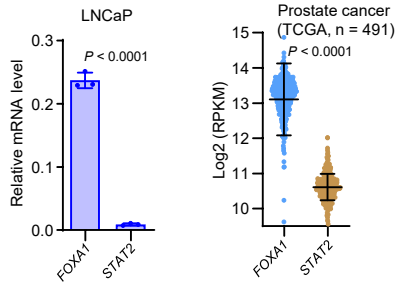

D

Sample	ChIP-seq	Total peaks	MEME-ChIP top hit motif	STAT2 binding peaks overlapped with FOXA1 peaks					
				STAT2 Up-peaks (n = 192)		STAT2 Down-peaks (n = 45)		STAT2 NSA-peak (n = 557)	
				Number	Ratio	Number	Ratio	Number	Ratio
LNCaP cell line	**FOXA1**	50,838	FOXA1 motif (E-value<1e-300) No potential STAT2 motif was found	10	5%	22	48%	128	22%
Primary prostate cancer patient tissue GSM4569882	**FOXA1**	12,379	FOXA1 motif (E-value=5.1e-046) No potential STAT2 motif was found	1	1%	12	26%	81	14%
Primary prostate cancer patient tissue GSM4569883	**FOXA1**	47,396	FOXA1 motif (E-value<1e-300) No potential STAT2 motif was found	4	2%	13	28%	64	11%
Primary prostate cancer patient tissue GSM4569884	**FOXA1**	40,180	FOXA1 motif (E-value=6.0e-189) No potential STAT2 motif was found	1	1%	14	31%	81	14%
Primary prostate cancer patient tissue GSM4569885	**FOXA1**	20,138	FOXA1 motif (E-value=1.1e-126) No potential STAT2 motif was found	3	1%	15	33%	74	13%
Primary prostate cancer patient tissue GSM4569886	**FOXA1**	14,616	FOXA1 motif (E-value=9.8e-050) No potential STAT2 motif was found	1	1%	13	28%	84	15%
Primary prostate cancer patient tissue GSM4569887	**FOXA1**	40,370	FOXA1 motif (E-value=1.2e-204) No potential STAT2 motif was found	4	2%	13	28%	74	13%
Primary prostate cancer patient tissue GSM4569888	**FOXA1**	25,100	FOXA1 motif (E-value=1.3e-218) No potential STAT2 motif was found	1	1%	12	26%	86	15%
Primary prostate cancer patient tissue GSM4569889	**FOXA1**	13,918	FOXA1 motif (E-value=1.7e-049) No potential STAT2 motif was found	1	1%	14	31%	82	14%
Primary prostate cancer patient tissue GSM4569890	**FOXA1**	64,140	FOXA1 motif (E-value<1e-300) No potential STAT2 motif was found	5	2%	15	33%	78	14%
Primary prostate cancer patient tissue GSM4569891	**FOXA1**	55,558	FOXA1 motif (E-value<1e-300) No potential STAT2 motif was found	3	1%	12	26%	65	11%
Primary prostate cancer patient tissue GSM4569892	**FOXA1**	12,639	FOXA1 motif (E-value=1.8e-079) No potential STAT2 motif was found	0	0%	15	33%	61	10%
Primary prostate cancer patient tissue GSM4569893	**FOXA1**	2,050	ZN502 motif (E-value=1.2e-087) No potential STAT2 motif was found	0	0%	15	33%	80	16%
Primary prostate cancer patient tissue GSM4569893	**FOXA1**	66,960	FOXA1 motif (E-value<1e-300) No potential STAT2 motif was found	11	5%	12	26%	63	11%

E

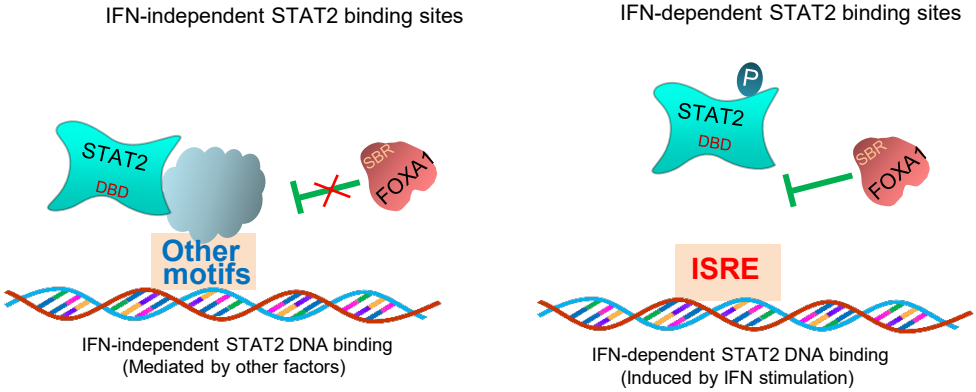

Supplementary Figure 8. Impact of IFNα treatment on FOXA1 occupancy on chromatin and genome-wide overlap between FOXA1 binding sites with STAT2 binding sites. (Related Figure 3)

A. The FOXA1 binding intensity (top) and binding signal heatmap (bottom) of FOXA1 binding sites in LNCaP cells treated with or without IFNα (100 ng/L).

B. Venn diagram shows the overlap of total FOXA1 binding peaks with Up-peaks, Down-peaks and NSA-peaks of STAT2 induced by FOXA1 KD in LNCaP treated with IFNα (100 ng/L). The top hit of the DNA motif defined by MEME-ChIP analysis in each group is also shown.

C. The relative expression level of *FOXA1* and STAT2 *mRNA* in LNCaP cells (Left, normalized to *GAPDH* mRNA expression level) and RNA-seq reads of *FOXA1* and STAT2 *mRNA* in primary PCa tissues of the TCGA cohort (Right). Data shown as means ± SD (n = 3, left; n = 491, right). Statistical comparison was done using Mann-Whitney U test.

D. Detailed information regarding the overlap of total FOXA1 binding peaks identified in LNCaP or 13 primary prostate cancer tissues with the Up-peaks, Down-peaks and NSA-peaks of STAT2 induced by FOXA1 KD in IFNα-treated LNCaP cells. Ratio of overlap = Numbers of overlapped peaks / Total STAT2 peaks of each cluster × 100%.

E. A hypothetical model deciphering FOXA1 overexpression-mediated suppression of IFN-dependent but not IFN-independent STAT2 DNA binding activity.

Supplementary Figure 9

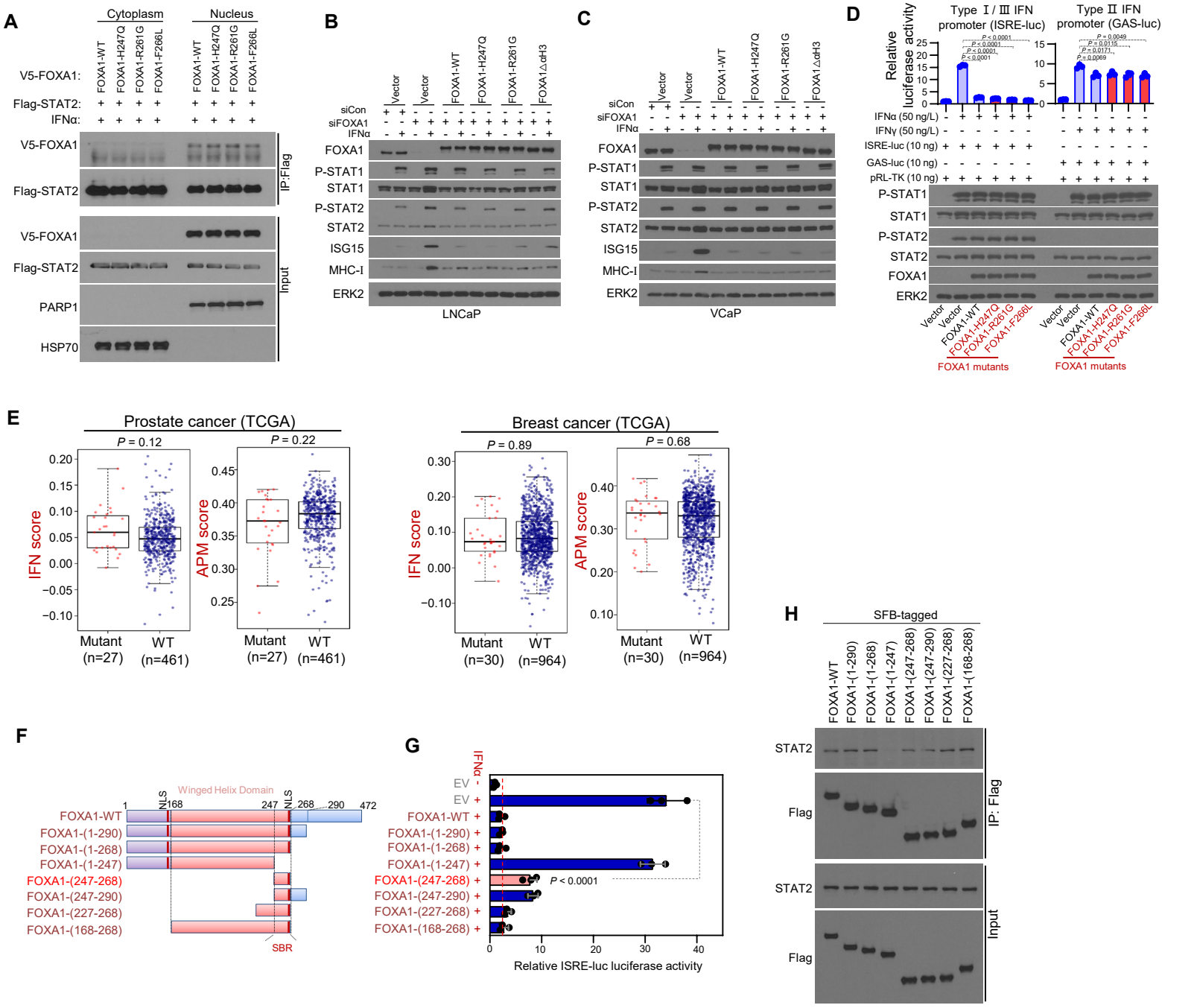

Supplementary Figure 9. Effects of PCa-derived FOXA1 mutants on the expression of IFN signature and APM genes. (Related to Figures 1-3)

A. Co-IP-based analysis of the interaction of ectopically expressed FOXA1-WT and PCa-associated mutants (FOXA1- H247Q, FOXA1-R261G and FOXA1-F266L) with STAT2 in 293T cells.

B. Western blot analysis of the effect of FOXA1 KD and restored expression of FOXA1 WT or PCa-derived mutants on IFNα-induced expression of IFN response genes in LNCaP PCa cell. ERK2, a loading control.

C. Western blot analysis of the effect of FOXA1 KD and restored expression of FOXA1 WT or PCa-derived mutants on IFNα-induced expression of IFN response genes in VCaP PCa cell. ERK2, a loading control.

D. Effects of FOXA1-WT and PCa-derived mutants FOXA1-H247Q, FOXA1-R261G and FOXA1-F266L on the activity of ISRE-luc and GAS-luc reporters in 293T cells treated with vehicle, IFNα or IFNγ. Data shown as means ± SD (n = 3); Statistical significance was determined by one-way ANOVA with Bonferroni correction for multiple tests.

E. Analysis of the association of FOXA1 mutations with the expression of IFN response genes (IFN score) and expression of antigen presentation machinery genes (APM score) in the TCGA cohorts of prostate and breast cancer. Data shown as means ± SD; Statistical comparison was done using Mann-Whitney U test.

F. Diagram shows the FOXA1 truncation expression constructs. NLS, nuclear localization signal; SBR, STAT2 binding region.

G. Luciferase reporter assay shows the inhibitory effect of the indicated FOXA1 WT or truncations on ISRE-luc reporter gene activity in DU145 cells. Data shown as means ± SD (n = 3). Statistical significance was determined by one-way ANOVA with Bonferroni correction for multiple tests.

H. Co-IP analysis of the interaction of SFB-tagged FOXA1 WT or truncations with STAT2 in 293T cells treated with IFNα.

Supplementary Figure 10

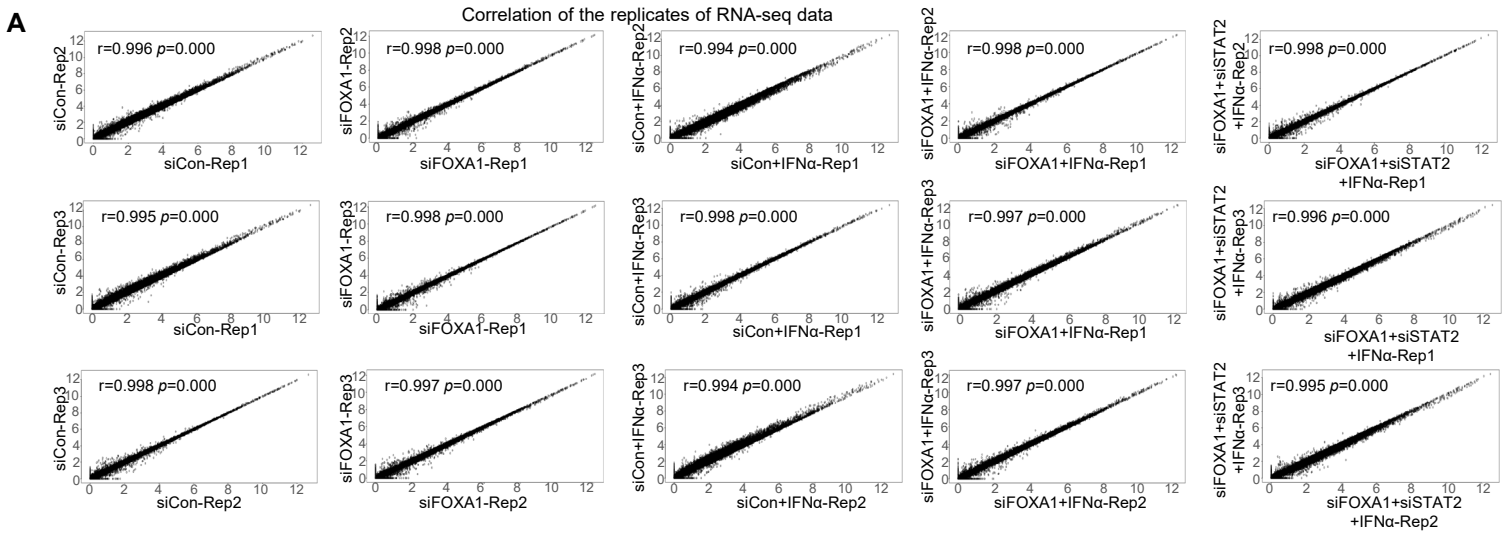

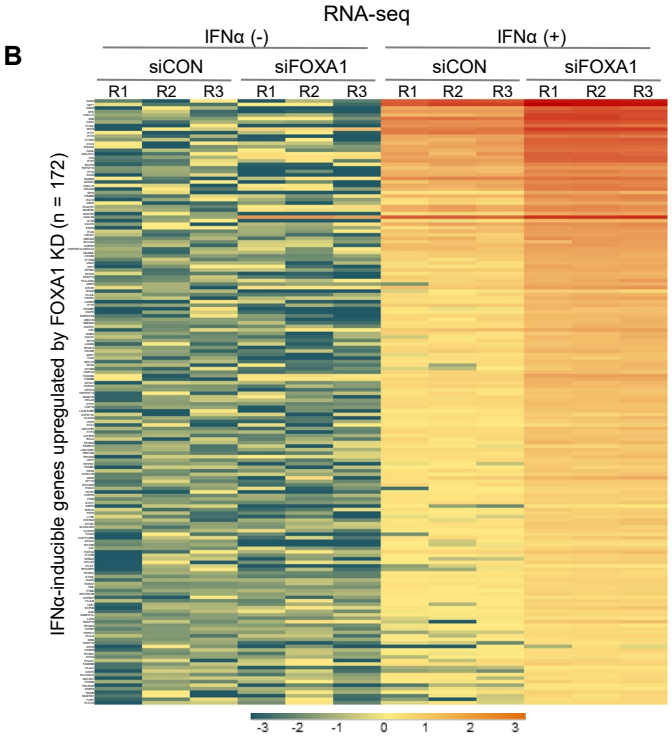

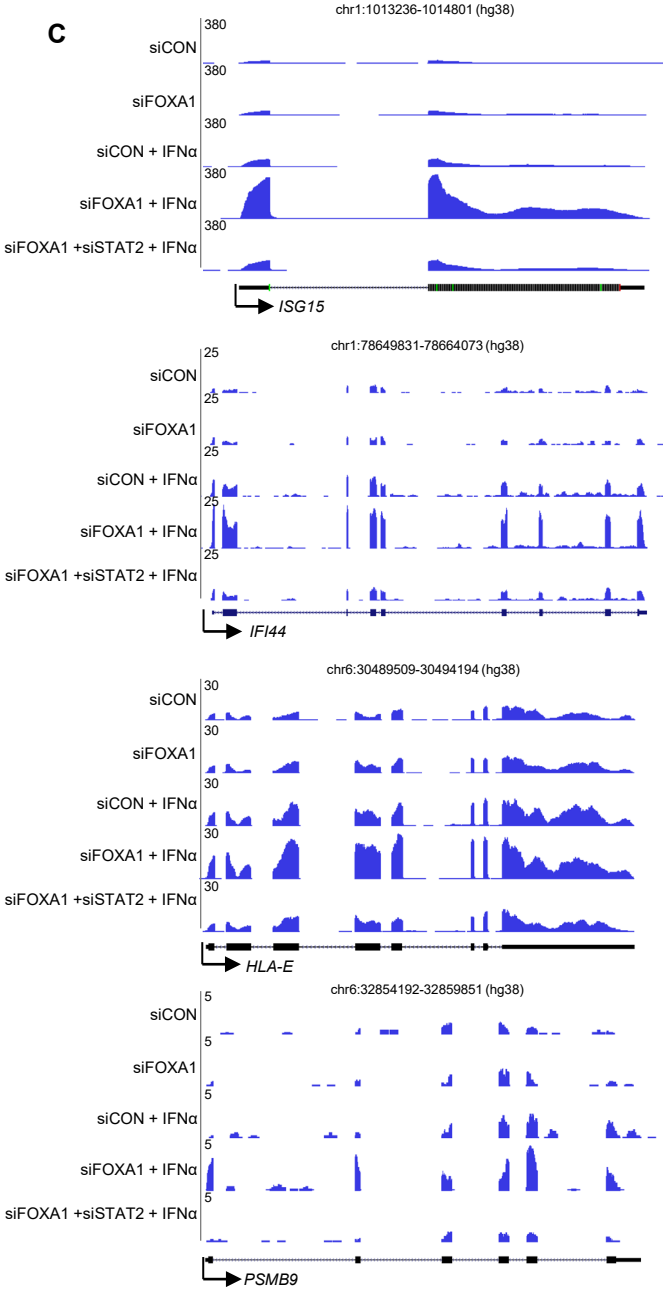

Supplementary Figure 10. Impact of IFNα treatment on STAT2 target gene expression. (Related Figure 4)

A. Analysis of correlation between the replicates for RNA-seq data in each indicated cellular condition.

B. Heatmaps of RNA-seq data showing a group of IFNα-inducible genes (n = 172) significantly upregulated ($P < 0.0001$) by FOXA1 KD in LNCaP cells. Statistical comparison was done using one-way analysis of variance (ANOVA).

C. UCSC tracks (integration of three replicates) show RNA-seq signals at genomic loci of STAT2 target genes *ISG15*, *IFI44*, *HLA-E* and *PSMB9*.

Supplementary Figure 11

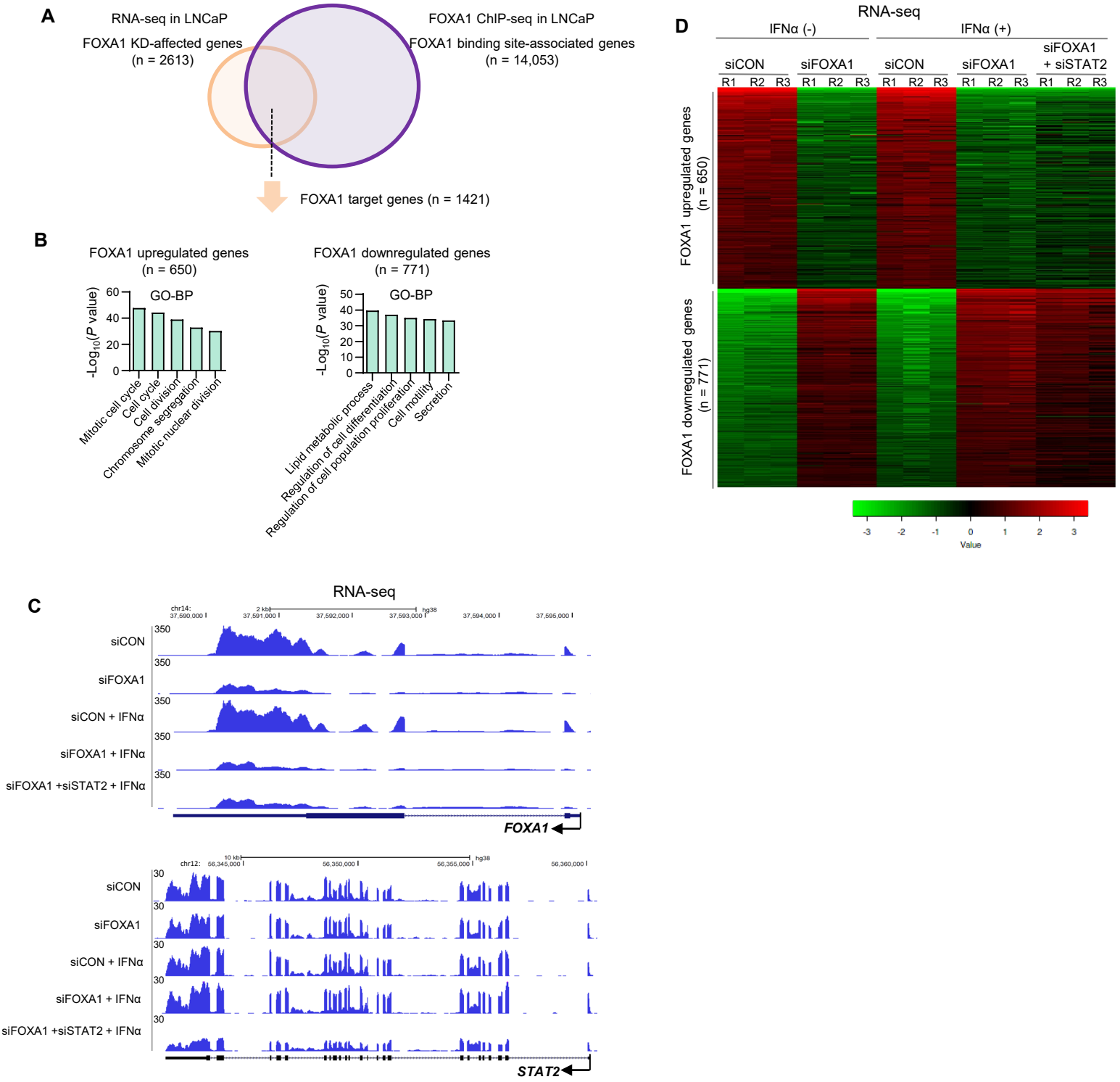

Supplementary Figure 11. Impact of IFNα treatment on FOXA1 target gene expression. (Related Figure 4)

A. Venn diagram shows the overlap between the genes affected by FOXA1 KD in LNCaP identified by RNA-seq and FOXA1 target genes identified by FOXA1 ChIP-seq in LNCaP cells.

B. GO-BP analysis shows the top 5 pathways of FOXA1-up- or down-regulated.

C. UCSC track profiles of RNA-seq signals at the *FOXA1* and *STAT2* gene loci in LNCaP cells transfected with siRNAs and/or treated with or without IFNα.

D. Heatmaps of RNA-seq data showing the expression of FOXA1 up- and down-regulated genes in LNCaP cells transfected with indicated siRNAs and/or treated with or without IFNα.

Supplementary Figure 12

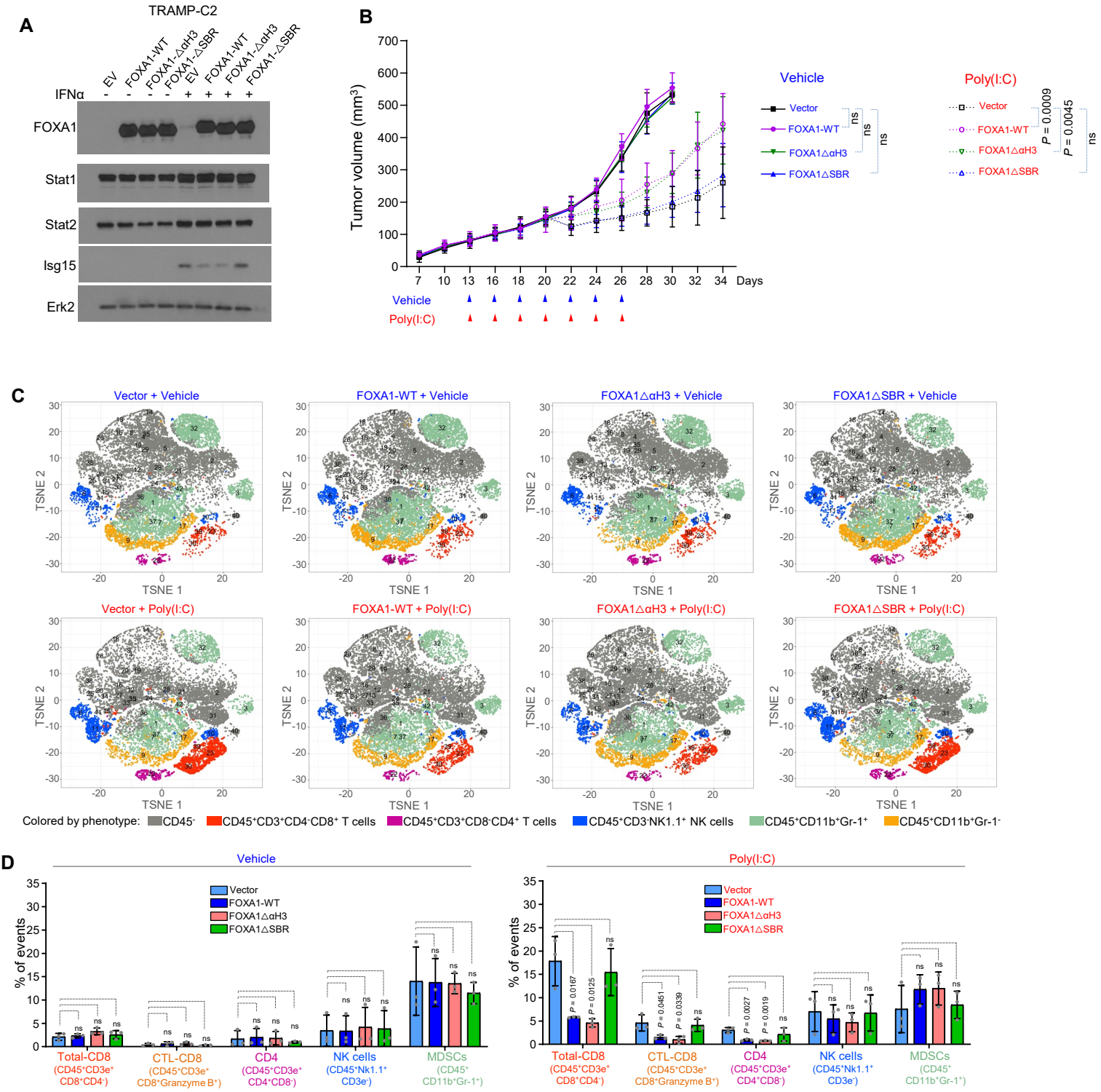

Supplementary Figure 12. FOXA1 overexpression suppresses PCa immune response in mice. (Related Figure 5)

A. Western blot analysis of indicated proteins in TRAMP-C2 murine PCa cells transfected with indicated expression vectors and treated with or without IFNα. Erk2, a loading control.

B. Growth of TRAMP-C2-Vector and TRAMP-C2-FOXA1-WT, TRAMP-C2-FOXA1ΔαH3 and TRAMP-C2-FOXA1ΔSBR tumors treated with or without Poly(I:C). The data are presented as the mean ± SD (n = 10). Statistical significance was determined by two-way analysis of variance (ANOVA).

C. CyTOF analysis of TRAMP-C2 murine PCa cells. PhenoGraph-defined cellular distribution and clustering, as defined by tSNE1 and tSNE2, colored by cellular phenotypes in TRAMP-C2 tumors stably expressing vector, FOXA1-WT, FOXA1ΔαH3 and FOXA1ΔSBR from mice at two days after the last administration of vehicle or Poly(I:C).

D. CyTOF analysis of TRAMP-C2 murine PCa cells. Data were derived from normalized viable single cells and analyzed with the PhenoGraph algorithm and are shown in the bar graphs as means ± SD (n = 3). Statistical significance was determined by one-way ANOVA with Bonferroni correction for multiple tests. CTL, cytotoxic T lymphocyte; NK, natural killer cells; MDSC, myeloid-derived suppressor cells.

Supplementary Figure 13

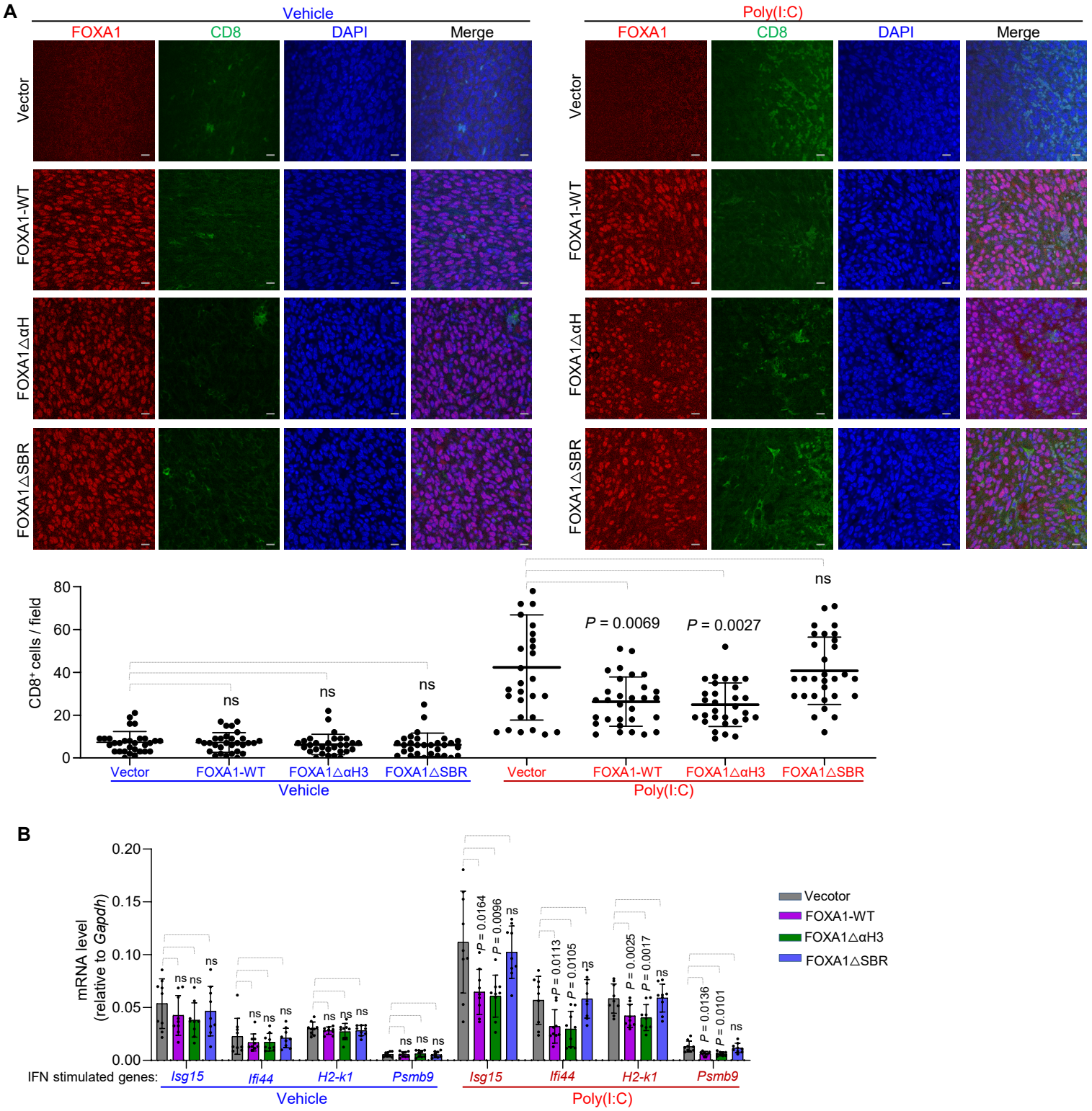

Supplementary Figure 13. FOXA1 inhibits immune response in mice. (Related to Figure 5)

A. Immunofluorescence chemistry analysis of expression of the transfected FOXA1-WT, FOXA1ΔαH3, FOXA1ΔSBR and CD8 in TRAMP-C2 tumors from mice at 2 day after the last administration of vehicle or poly(I:C). $CD8^+$ cells were quantified in 10 randomly selected fields from tumor section; Scale bar,10μm. The data are presented as the mean ± SD from 3 tumors (n = 30 fields). Statistical significance was determined by one-way ANOVA with Bonferroni correction for multiple tests.

B. RT-qPCR analysis of STAT2 target genes *Isg15*, *Ifi44*, *H2-k1* and *Psmb9* in TRAMP-C2 tumors transfected empty vector, FOXA1-WT, FOXA1ΔαH3 or FOXA1ΔSBR at 2 day after the last administration of vehicle or poly(I:C). The data are presented as the mean± SD (n = 9); Statistical significance was determined by one-way ANOVA with Bonferroni correction for multiple tests.

Supplementary Figure 14

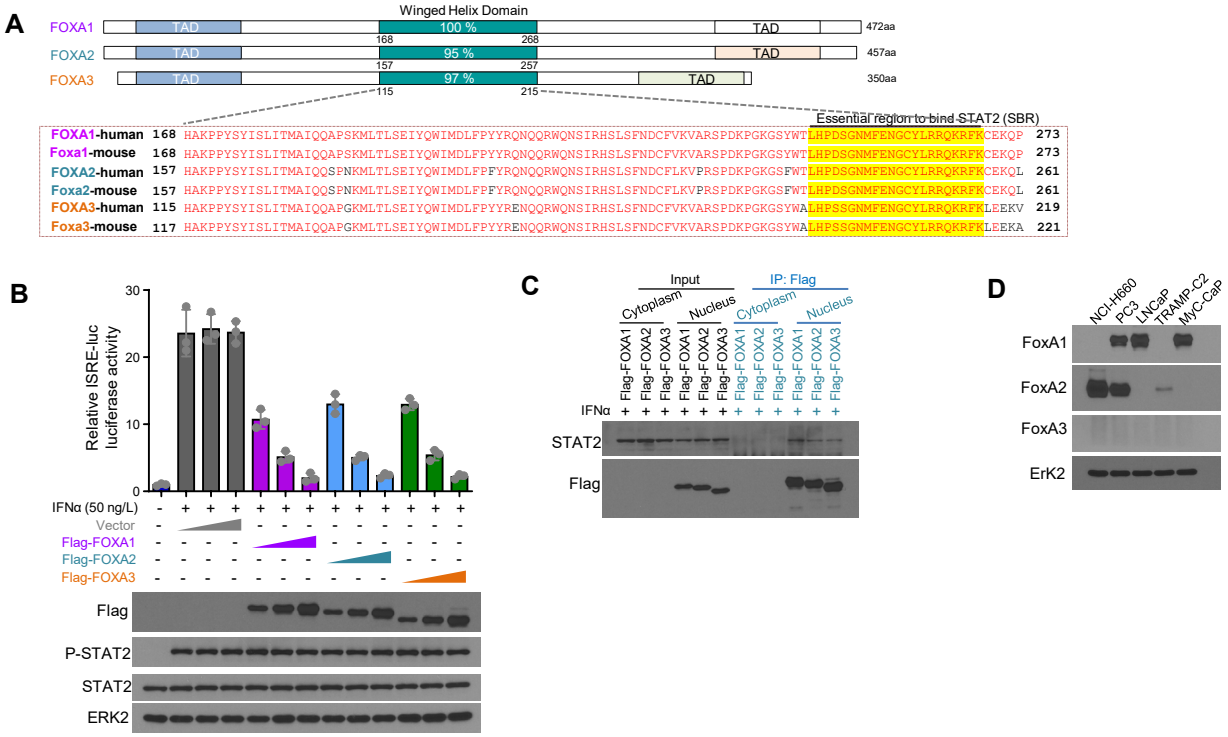

Supplementary Figure 14. Assessment of the IFN inhibitory effect of FOXA1, FOXA2 and FOXA3. (Related to Figures 5)

A. Diagram shows the domain structure and similarity of Winged Helix domain in the indicated FOX-proteins.

B. Luciferase reporter assay shows the inhibitory effect of different dose of FOXA1, FOXA2 and FOXA3 on ISRE-luc reporter gene activity in DU145 cells. Data shown as means ± SD (n = 3).

C. Co-IP analysis of the interaction of Flag-tagged FOXA1, FOXA2 and FOXA3 with STAT2 in 293T cells treated with IFNα.

D. Western blot analysis of expression of FOXA1, FOXA2, FOXA3 proteins in the indicated cell lines. ERK2 was used as a loading control.

Supplementary Figure 15

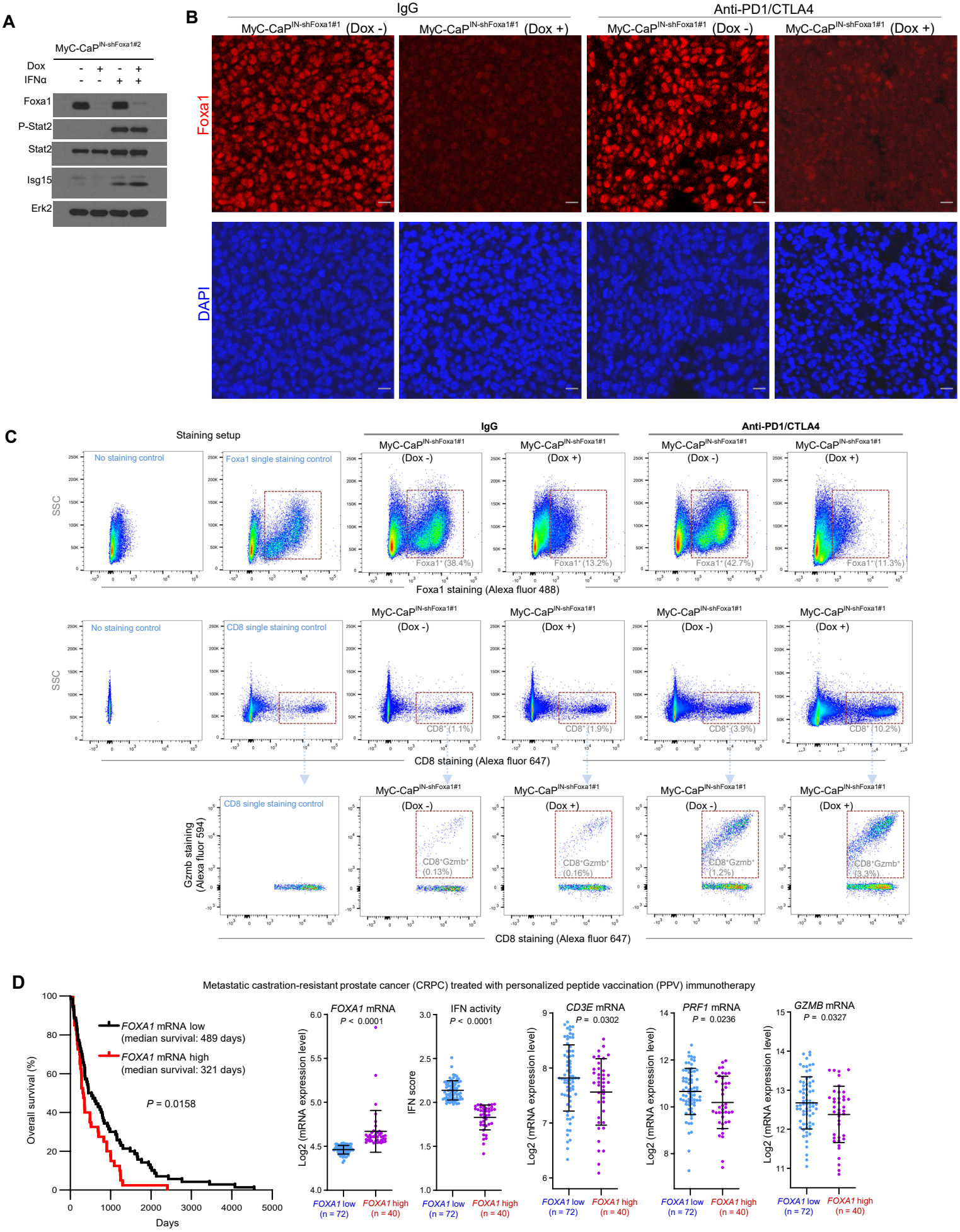

Supplementary Figure 15. Foxa1 inhibits immune response in mice and in patient of PCa. (Related to Figure 6)

A. Western blot analysis of indicated proteins in MyC-CaP murine PCa cells stably expressing doxycycline-inducible lentiviral shFoxa1#2 (MyC-CaP$^{IN\text{-}shFoxa1\#2}$) and treated with or without doxycycline (Dox) or/and IFNα. Erk2, a loading control.

B. Immunofluorescence chemistry analysis of expression of the transfected Foxa1 in MyC-CaP$^{IN\text{-}shFoxa1\#1}$ tumors from mice at 2 day after the last administration of IgG or Anti-PD1/CTLA4; Scale bar, 10 μm.

C. Flow cytometry analysis of Foxa1, CD8 and Gzmb positive cells in MyC-CaP$^{IN\text{-}shFoxa1\#1}$ tumors from mice at two days after the last administration of IgG or anti-PD1/CTLA-4. Dox (-), without doxycycline treatment; Dox (+), with doxycycline treatment.

D. Overall survival of patients with *FOXA1*-low or -high PCa treated with personalized peptide vaccination (PPV) immunotherapy. Analysis of microarray data (GSE53922) from this cohort of patients shows the inverse correlation of *FOXA1* expression with the IFN activity and expression of *CD3E*, *CD8A* and *GZMB* genes. The mean value of *FOXA1* expression level was used as the cutoff. Statistical significance was determined by Log-rank (Mantel-Cox) test for overall survival and the others by Mann-Whitney U test.

Supplementary Figure 16

A

Breast cancer treated with NAC (Mayo Clinic cohort, n = 128)

Clinical molecular subtype		pCR	No-pCR
Lum A (n = 11)		0 (0%)	11 (100%)
Lum B (n = 37)		4 (10.8%)	33 (89.2%)
Lum unknown (n = 2)		0 (0%)	2 (100%)
$ER^+/HER2^+$ (n=16)		4 (25%)	12 (75%)
$ER^-/HER2^+$ (n = 20)		12 (60%)	8 (40%)
TNBC	LAR (n = 6)	1 (16%)	5 (84%)
	Basal-like (n = 36)	23 (64%)	13 (36%)

B

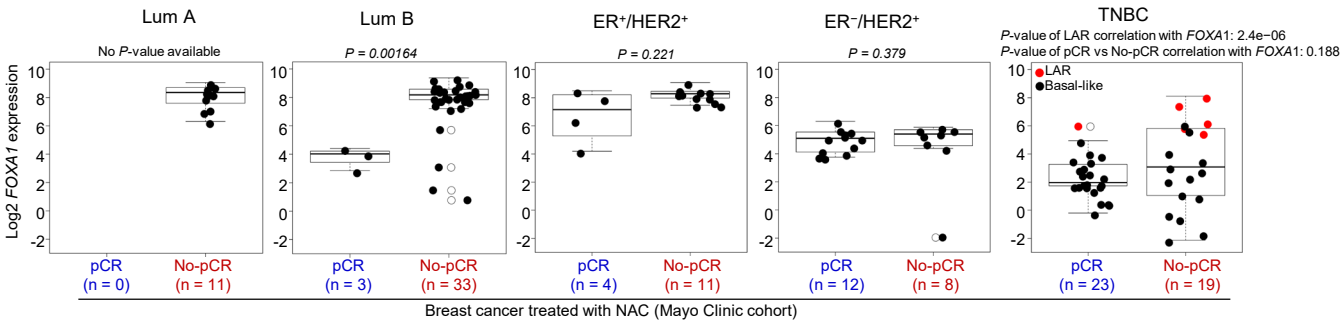

C

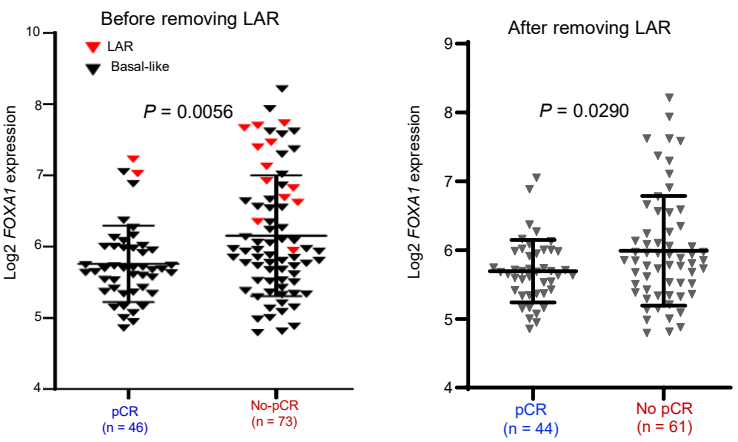

D

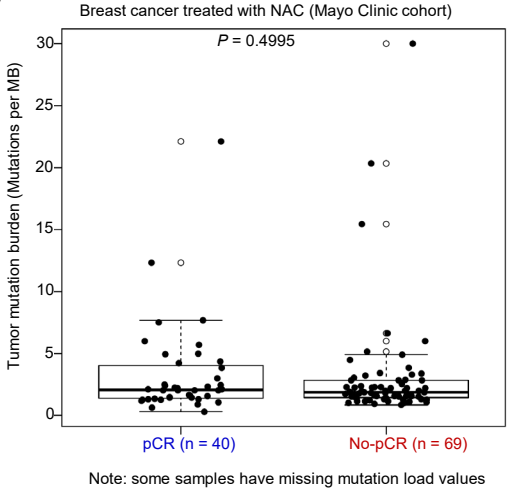

Note: some samples have missing mutation load values

E

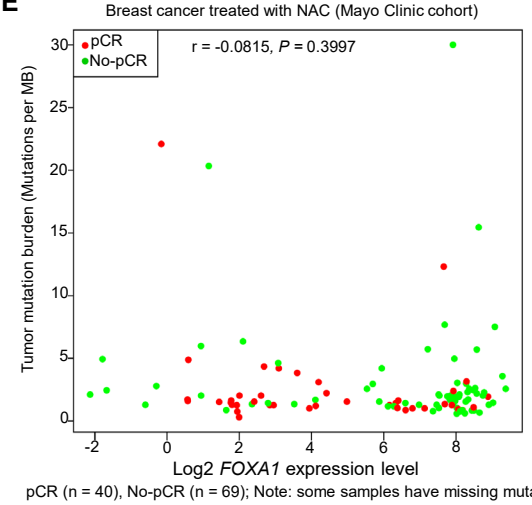

pCR (n = 40), No-pCR (n = 69); Note: some samples have missing mutation load values

Supplementary Figure 16. Assessment of inverse correlation between *FOXA1* expression and responsiveness to NAC in molecular subtypes of breast cancer. (Related to Figure 7)

A. The number of cases of breast cancers in different molecular subtypes (from a cohort of patients of the Mayo Clinic) with pathological complete response (pCR) or No-pCR to neoadjuvant chemotherapy (NAC).

B. Comparison of *FOXA1* expression level in luminal A (Lum A), luminal B (Lum B), $ER^+/HER2^+$, $ER^-/HER2^+$, and TNBC (LAR or basal-like) tumors (from the Mayo Clinic cohort of patients) with pathological complete response (pCR) or No-pCR to NAC. Data shown as means $\pm$ SD; Statistical comparison was done using Mann-Whitney U test.

C. Analysis of microarray data shows the association of FOXA1 expression in a cohort of TNBC tumors (GSE106977) with pCR or No-pCR to NAC. Right, before removing luminal AR (LAR); Left, after removing luminal AR (LAR). Data shown as means $\pm$ SD; Statistical comparison was done using Mann-Whitney U test.

D. Analysis of the association of DNA mutation burden in the cohort of 126 BCa samples from Mayo Clinic with tumors response to NAC (pCR versus No-pCR). Data shown as means $\pm$ SD; Statistical significance was determined by Mann-Whitney U test.

E. Analysis of the association of DNA mutation burden in the cohort of 126 BCa samples from Mayo Clinic with tumors response to *FOXA1* expression levels. Statistical significance was determined by Pearson correlation test.

Supplementary Figure 17

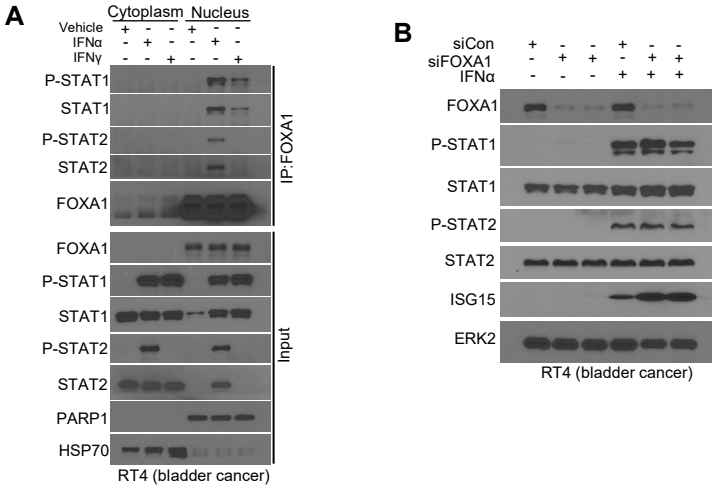

Supplementary Figure 17. The effect of FOXA1 on IFN signaling in bladder cancer. (Related to Figure 8)

A. Co-IP analysis of FOXA1 interaction with STAT1 and STAT2 at the endogenous level in RT4 bladder cancer cells after treatment of IFNα or IFNγ.

B. Western blot analysis of the indicated proteins in RT4 bladder cancer cells transfected with control siRNA (siCon) or FOXA1 specific siRNA (siFOXA1) and/or treated with or without IFNα.

Supplementary Figure 18

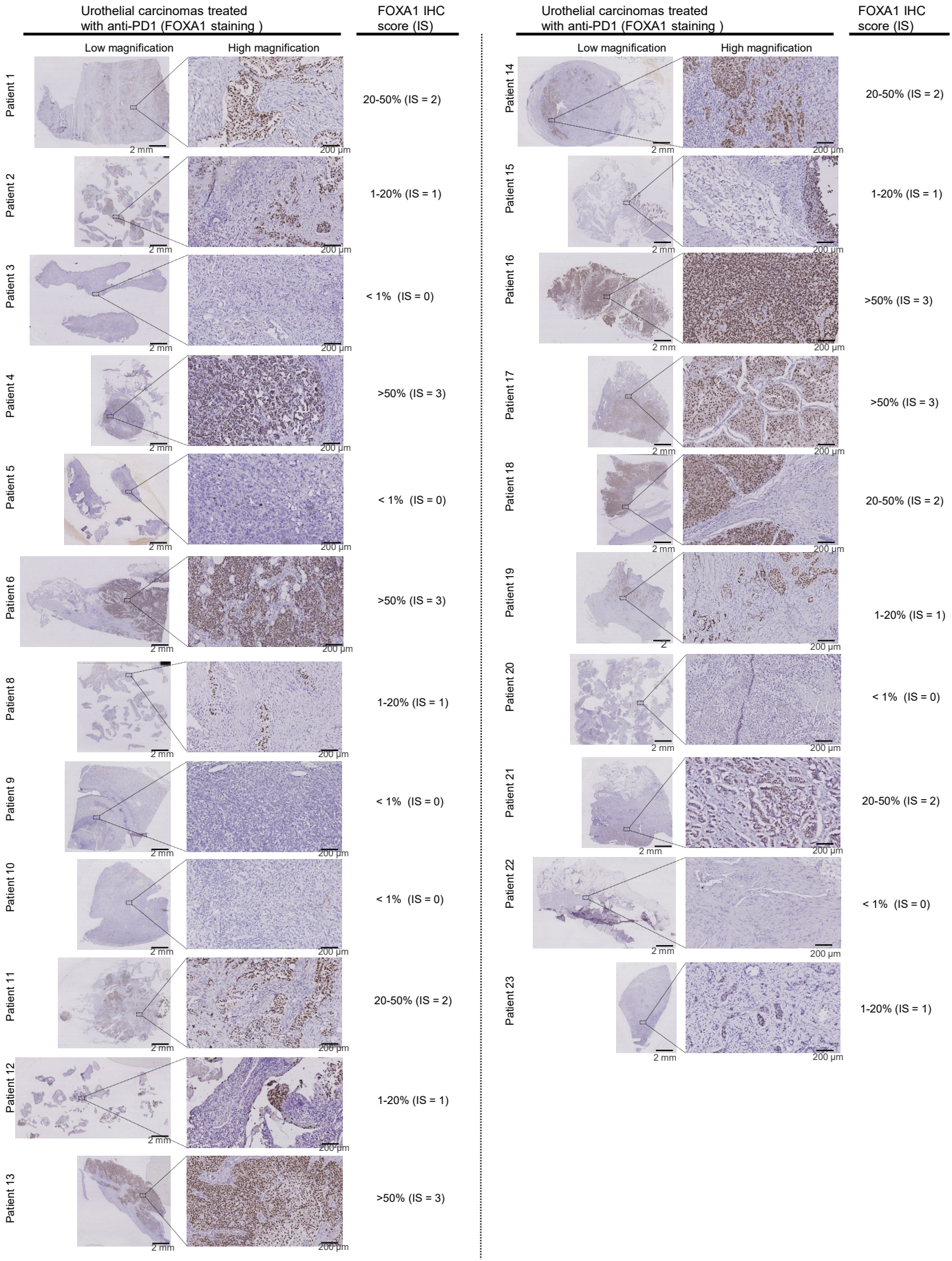

Supplementary Figure 18. IHC analysis of FOXA1 protein expression in pre-treatment urothelial carcinoma specimens from a cohort of patients treated with anti-PD1 immunotherapy. (Related to Figure 8)

FOXA1 IHC was performed using a FOXA1-specific antibody on pre-treatment urothelial carcinoma specimens from a cohort of 22 patients treated with anti-PD1 immunotherapy. Low and high magnification FOXA1 IHC images in each case and FOXA1 IHC scores are shown (see scoring details in Supplementary Methods and in Supplementary Table 3). Scale bars: 2 mm (low magnification); 200 µm (high magnification).

Supplementary Figure 19

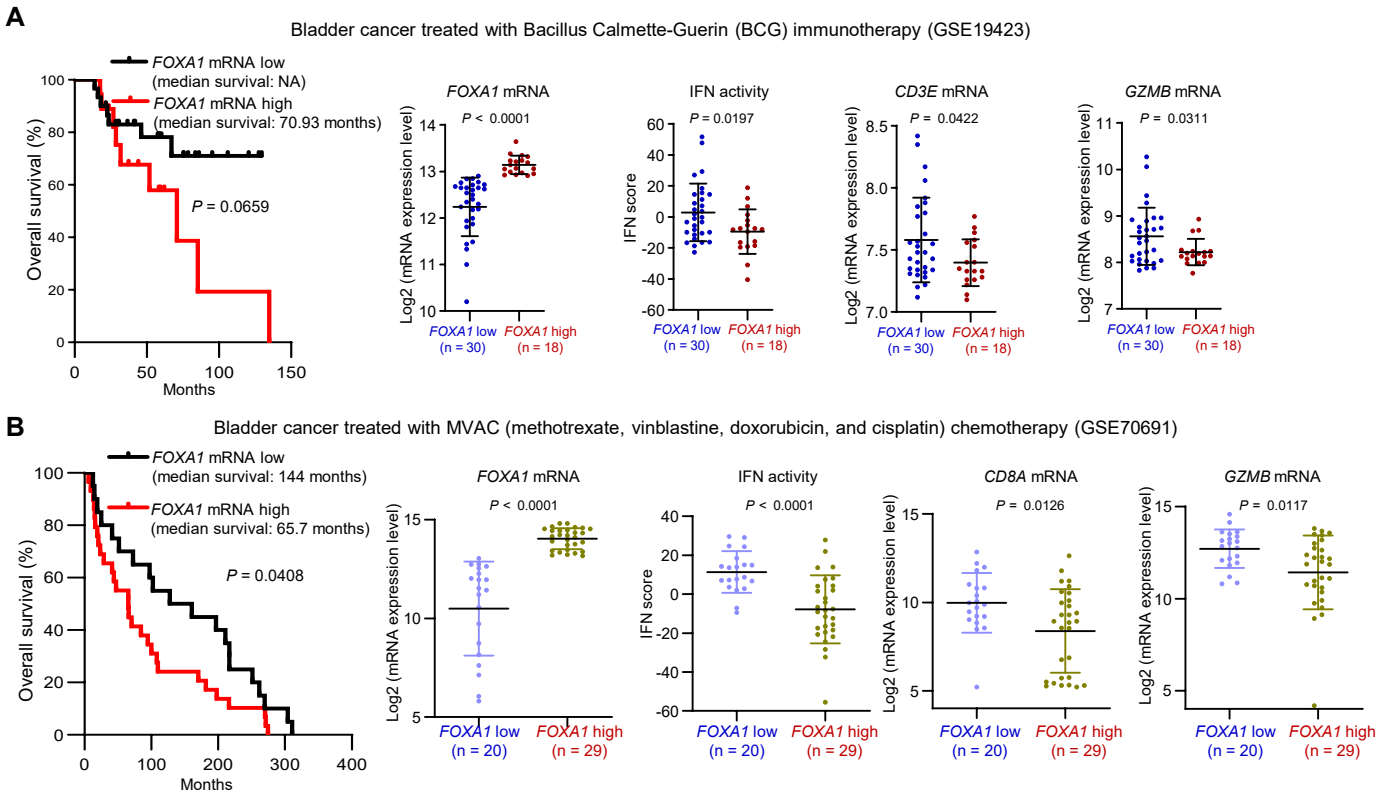

Supplementary Figure 19. FOXA1 confers to immunotherapy and chemotherapy resistance in bladder cancer. (Related to Figure 8)

A. Overall survival of patients with FOXA1-low or -high bladder cancer treated with Bacillus Calmette-Guerin (BCG) immunotherapy. Analysis of microarray data (GSE19423) from this cohort of patients shows the inverse correlation of *FOXA1* expression with the IFN activity and expression of *CD3E*, *CD8A* and *GZMB* T cell marker genes. The mean value of *FOXA1* expression level was used as the cutoff. Statistical significance was determined by Log-rank (Mantel-Cox) test for overall survival and the others by Mann-Whitney U test. NA = Not available.

B. Overall survival of patients with FOXA1-low or -high bladder cancer treated with methotrexate, vinblastine, doxorubicin, and cisplatin (MVAC) chemotherapy. Analysis of microarray data (GSE70691) from this cohort of patients shows the inverse correlation of *FOXA1* expression with the IFN activity and expression of *CD3E*, *CD8A* and *GZMB* T cell marker genes. The mean value of *FOXA1* expression level was used as the cutoff. Statistical significance was determined by Log-rank (Mantel-Cox) test for overall survival and the others by Mann-Whitney U test.

Supplementary Table 1. Clinic information of prostate cancer samples used for single cell RNA-seq.

Sample ID	Gleason score	WHO/ISUP	Tumor cellularity	pre-operative PSA (ng/mL)	Clinical T	Clinical N	Clinical M	pT	pN	Neoadjuvant ADT
Patient 1	4+5	5	60%	79.44	T4	N1	M0	T3b	N1	NO
Patient 2	5+5	5	70%	18.51	T4	N0	M0	T3b	N0	NO
Patient 3	4+5	5	80%	7.05	T3a	N0	M0	T3b	N0	NO
Patient 4	4+5	5	80%	22.57	T3a	N0	M0	T3a	N0	NO
Patient 5	4+3	3	80%	10.50	T2c	N0	M0	T2c	N0	NO
Patient 6	4+3	3	90%	336.00	T2c	N1	M0	T3b	N1	NO
Patient 7	4+5	5	10%	16.00	T2c	N1	M1b	T2c	N1	NO
Patient 8	4+5	5	70%	16.00	T2c	N1	M1b	T2c	N1	NO
Patient 9	4+5	5	90%	20.00	T2c	N0	M0	T2c	N0	YES
Patient 10	3+4	2	60%	81.09	T2c	N0	M0	T2c	N0	NO
Patient 11	4+5	5	80%	19.00	T3a	N0	M1b	T3a	N0	NO
Patient 12	4+3	3	80%	51.00	T3a	N0	M0	T3a	N0	NO
Patient 13	4+5	5	50%	14.00	T2b	N0	M1a	T3a	N0	NO

Supplementary Table 2. Single cell RNA-seq information of prostate cancer patients used for analysis.

Sample ID	Average_nGene	Average_nUMI	Average_percent.mito	Cell_Number	Epithelia_Cell
Patient 1	2864.398856	14306.05616	0.082028703	1923	668
Patient 2	466.7349769	874.4571135	0.055694131	1947	335
Patient 3	2026.572198	8897.319504	0.104496127	3712	963
Patient 4	3034.626333	14956.16967	0.074302536	6000	5694
Patient 5	1360.559574	5324.886525	0.30085929	4230	1374
Patient 6	1543.450465	5390.983189	0.074496791	6127	3688
Patient 7	557.5352157	1272.217322	0.053934186	3152	951
Patient 8	1970.975065	8287.448083	0.104352916	5374	2852
Patient 9	1160.757277	4373.853596	0.097172687	2336	262
Patient 10	2399.793621	9504.188793	0.07756701	5800	2129
Patient 11	1651.909848	6503.126894	0.184457406	2640	798
Patient 12	1469.374933	6327.621578	0.144288349	3726	1014
Patient 13	2037.840928	8201.765801	0.217854816	6123	2946

Supplementary Table 3. FOXA1 IHC staining of urothelial carcinoma with anti-PD1 treatment (see FOXA1 staining data in Supplementary Figure 18).

Patient ID	Cancer type	Pathological type	Gender (M = male; F = female)	Age (Years)	Disease progression (1 = Yes, 0 = No)	Progression free survival time (Days)	FOXA1 staining score (0 = "< 1%", 1 = "1-20%", 2 = "20-50%", 3 = ">50%")
1	bladder cancer	urothelial carcinoma	M	54	1	111	2
2	bladder cancer	urothelial carcinoma	M	67	0	927	1
3	bladder cancer	urothelial carcinoma	M	44	0	196	0
4	bladder cancer	urothelial carcinoma	M	51	1	112	3
5	bladder cancer	urothelial carcinoma	M	66	0	296	0
6	ureteral cancer	urothelial carcinoma	M	77	1	251	3
8	bladder cancer	urothelial carcinoma	M	73	1	207	1
9	renal pelvis urothelial carcinoma	urothelial carcinoma	F	47	0	128	0
10	renal pelvis urothelial carcinoma	urothelial carcinoma	M	64	0	50	0
11	bladder cancer	urothelial carcinoma	M	62	1	52	2
12	bladder cancer	urothelial carcinoma	M	68	1	40	1
13	ureteral cancer	urothelial carcinoma	F	71	1	70	3
14	ureteral cancer	urothelial carcinoma	M	71	1	54	2
15	bladder cancer	urothelial carcinoma	M	70	1	55	1
16	bladder cancer	urothelial carcinoma	M	62	1	55	3
17	renal pelvis urothelial carcinoma	urothelial carcinoma	F	66	1	60	3
18	bladder cancer	urothelial carcinoma	M	66	1	23	2
19	ureteral cancer	urothelial carcinoma	M	65	1	65	1
20	ureteral cancer	urothelial carcinoma	M	68	0	51	0
21	bladder cancer	urothelial carcinoma	M	48	0	36	2
22	bladder cancer	urothelial carcinoma	M	63	1	21	0
23	renal pelvis urothelial carcinoma	urothelial carcinoma	M	56	0	219	1

Supplementary Table 4. Primers for RT-qPCR and ChIP-qPCR.

Names	Sequence (5'-3')	Used for
GAPDH-F	CCGGGAAACTGTGGCGTGATGG	RT-qPCR
GAPDH-R:	AGGTGGAGGAGTGGGTGTCGCTGTT	RT-qPCR
FOXA1-F:	AGATGGAAGGGCATGAAACCA	RT-qPCR
FOXA1-R:	ATGTTGCCGCTCGTAGTCAT	RT-qPCR
STAT2-F	GAGGAGAAGCAATGGGTCTTAG	RT-qPCR
STAT2-R	GGTCCACAACCAACGAATAGA	RT-qPCR
IFI27-F:	GTTCATCCTGGGCTCCATTG	RT-qPCR
IFI27-R:	CCCCTGGCATGGTTCTCTT	RT-qPCR
HLA-E-F	CCTACGACGGCAAGGA	RT-qPCR
HLA-E-R	CCCTTCTCCAGGTATTTGTG	RT-qPCR
PSMB9-F	GAGAGGACTTGTCTGCACATC	RT-qPCR
PSMB9-R	GCATCCACATAACCATAGATAAAGG	RT-qPCR
IFI44-F	TGGTACATGTGGCTTTGCTC	RT-qPCR
IFI44-R	CCACCGAGATGTCAGAAAGAG	RT-qPCR
IFI44L-F	TGCACTGAGGCAGATGCTGCG	RT-qPCR
IFI44L-R	TCATTGCGGCACACCAGTACAG	RT-qPCR
IFI16-F	ACTGAGTACAACAAAGCCATTTGA	RT-qPCR
IFI16-R	TTGTGACATTGTCCTGTCCCCAC	RT-qPCR
PSMB9-F	GAGAGGACTTGTCTGCACATC	RT-qPCR
PSMB9-R	GCATCCACATAACCATAGATAAAGG	RT-qPCR
ISG15-F	GCGCAGATCACCCAGAAGAT	RT-qPCR
ISG15-R	TCCTCACCAGGATGCTCAGA	RT-qPCR
Gapdh-F:	TGGAAAGCTGTGGCGTGAT	RT-qPCR
Gapdh-R:	TGCTTCACCACCTTCTTGAT	RT-qPCR
Foxa1-F:	TCCTTATGGCGCTACCTTGC	RT-qPCR
Foxa1-R:	CCTTGGTAGTAGGCTGGCTC	RT-qPCR
Isg15-F:	AAGCAGCCAGAAGCAGACTC	RT-qPCR
Isg15-R:	CACCAATCTTCTGGGCAATC	RT-qPCR
Ifi44-F:	AACTGACTGCTCGCAATAATGT	RT-qPCR
Ifi44-R:	GTAACACAGCAATGCCTCTTGT	RT-qPCR
Psmb9-F:	ACCGTGAGGACTTGTTAGCG	RT-qPCR
Psmb9-R:	GTAAAGGGCTGTCGAATTAGCA	RT-qPCR
H2-k1-F:	CCGCGGACGCTGGATA	RT-qPCR
H2-k1-R:	GGCGATTCGCGACTTCTG	RT-qPCR
ISG15-F:	TGCATCCTGTGAAGGATCTG	ChIP-qPCR
ISG15-R:	TTTGGCTTCAGTTTCGGTTT	ChIP-qPCR
IFI44-F:	TGAGAGAAGTTGGCATGCTG	ChIP-qPCR
IFI44-R:	AGCTGAGGGTAGCTGCTCTGT	ChIP-qPCR
HLA-E-F:	GCCCAGCCAGGACTAATTTC	ChIP-qPCR
HLA-E-R:	CACCCATTGGGAATGAGAAC	ChIP-qPCR
PSMB9-F:	CCGAGTCCTCCCCTACTGG	ChIP-qPCR
PSMB-R:	GCAGGCCACTTTTGGAAGTA	ChIP-qPCR

Supplementary Table 5. Antibodies used for CyTOF.

Antibodies	Clone	Tag	Source	Localization
Anti-Mouse CD45	30-F11	89Y	Fluidigm, Cat#: 3089005B	surface
Anti-Mouse CD3e	145-2C11	152Sm	Fluidigm, Cat#: 3152004B	surface
Anti-Mouse CD8a	53-6.7	153-Eu	Fluidigm, Cat#: 3153012B	surface
Anti-Mouse CD4	RM4-5	145-Nd	Fluidigm, Cat#: 3145002B	surface
Anti-Mouse CD11b	M1/70	172-Yb	Fluidigm Cat#: 3172012B	surface
Anti-Mouse NK1.1	PK136	170Er	Fluidigm, Cat#: 3170002B	surface
Anti-Mouse Ly-6G	1A8	141Pr	Fluidigm, Cat#: 3141008B	surface
Anti-Mouse Ly-6C	HK1.4	162Dy	Fluidigm, Cat#: 3162014B	surface
Anti-Mouse Foxp3	FJK-16s	158Gd	Fluidigm, Cat#: 3158003A	intracellular
Anti-Mouse Granzyme B	GB11	173Yb	Fluidigm, Cat#: 3173006B	intracellular

Full unedited gel and blot images

Figure 2B, left

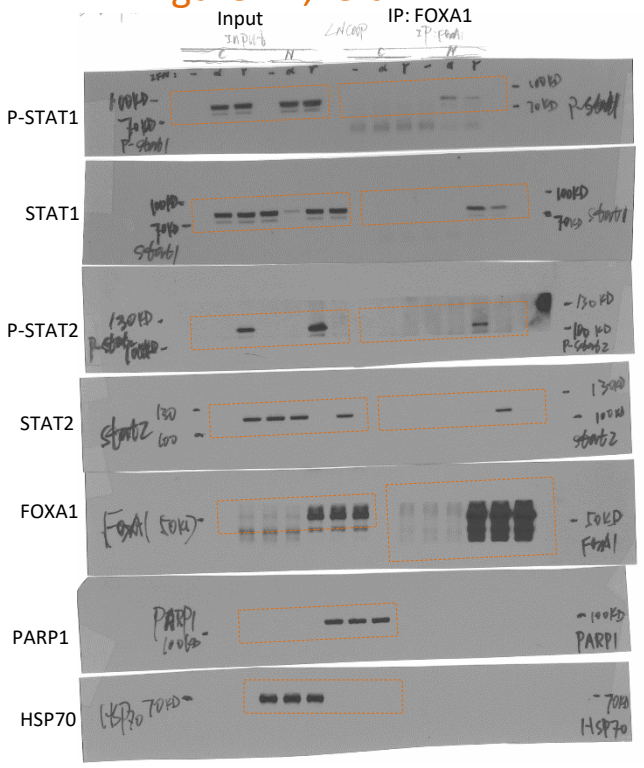

Figure 2B, right

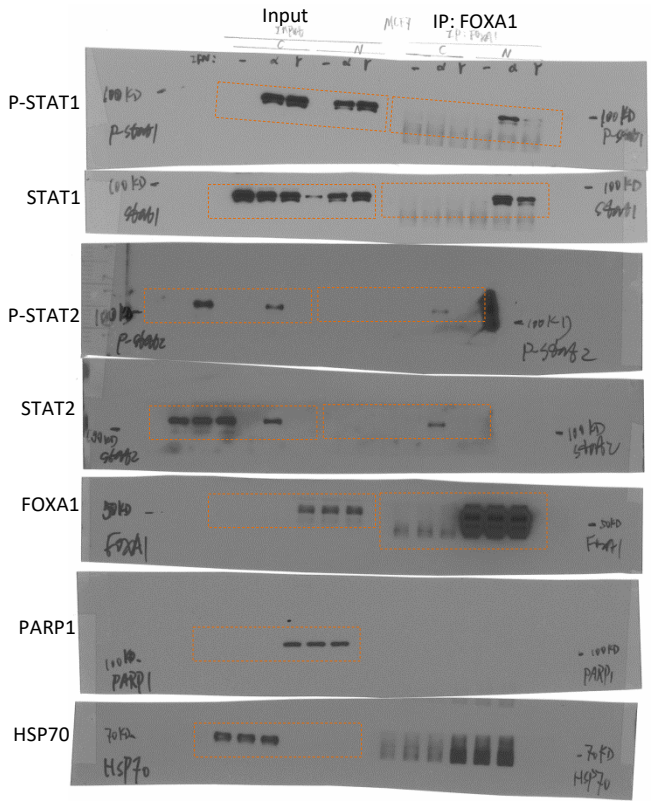

Figure 2C

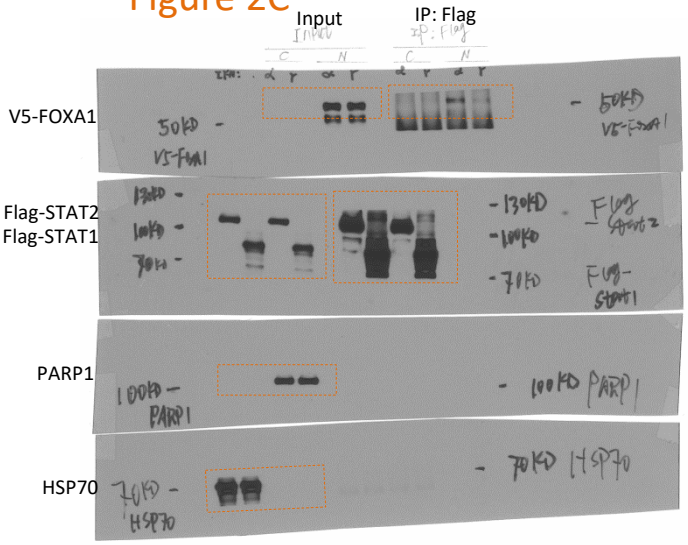

Figure 2E

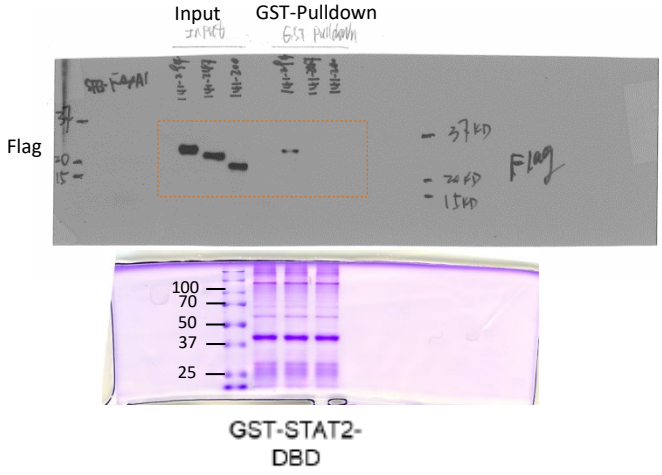

Figure 2F

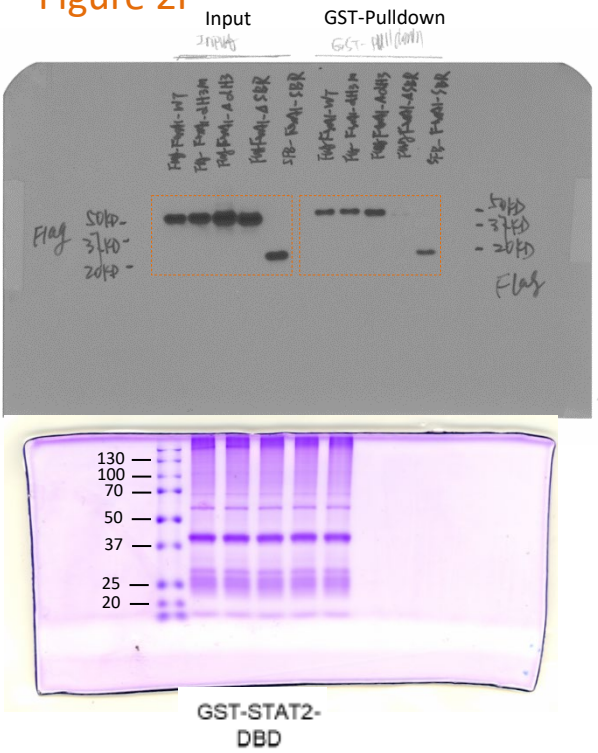

Figure 2G

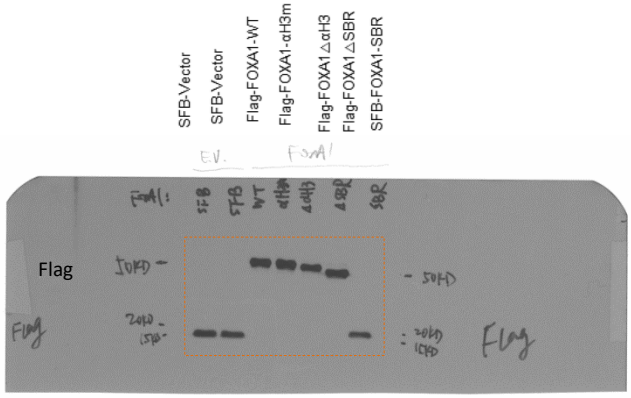

Figure 6A

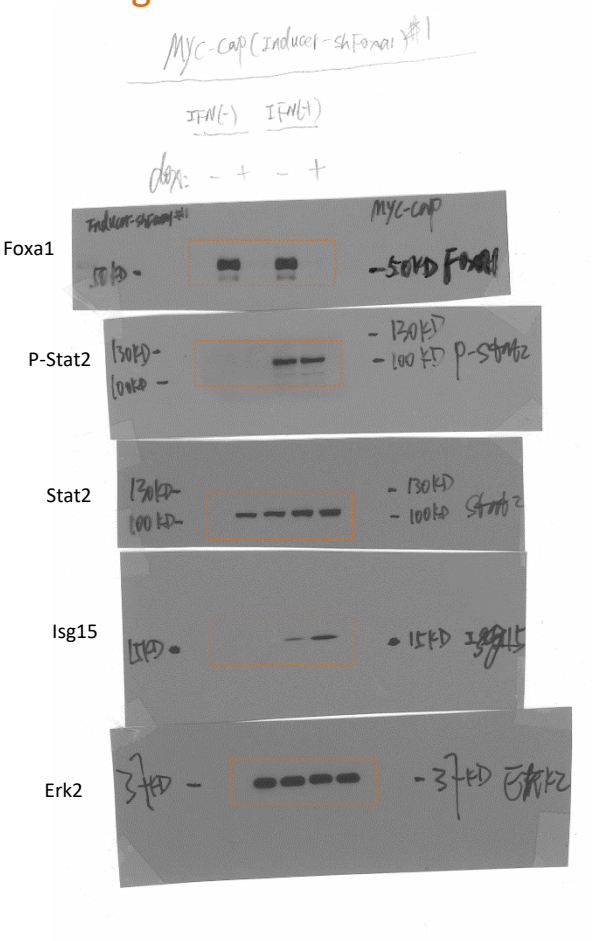

Figure S5A

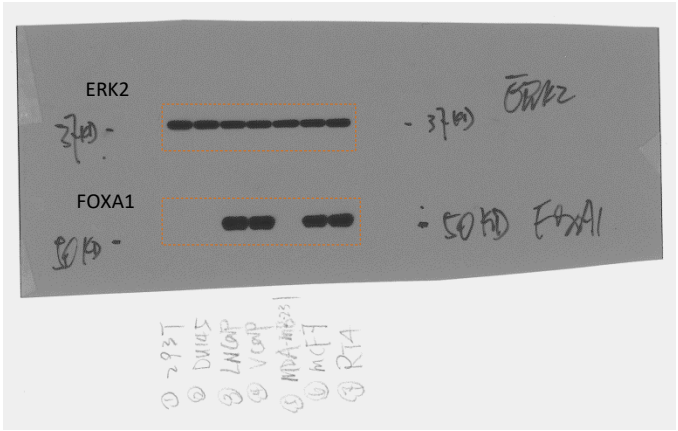

Figure S5B, left

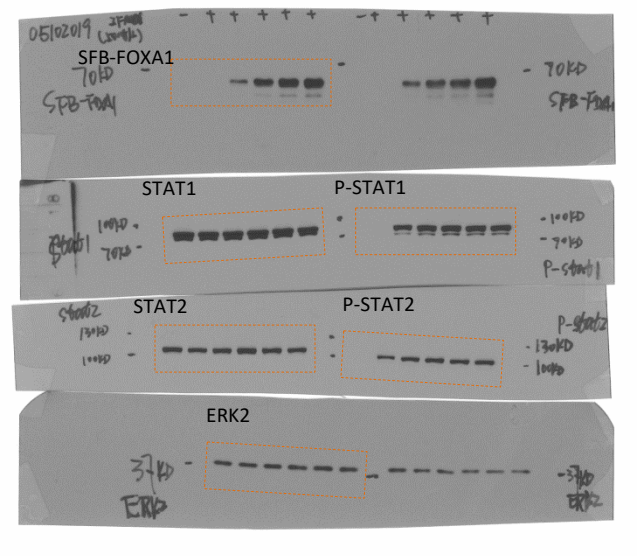

Figure S5B, right

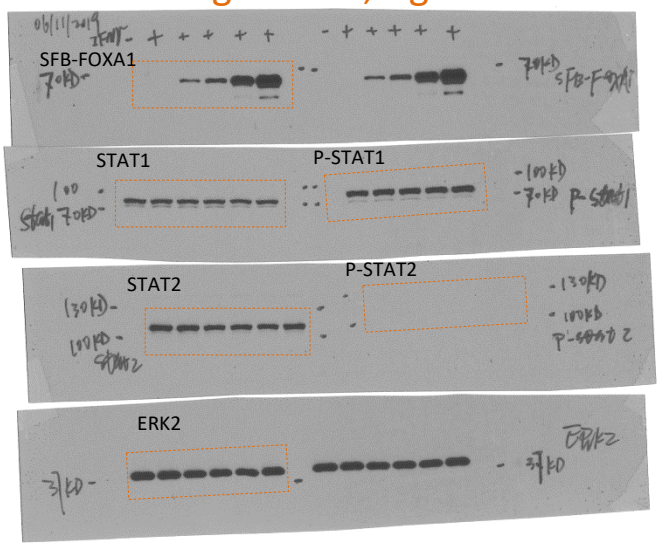

Figure S5C

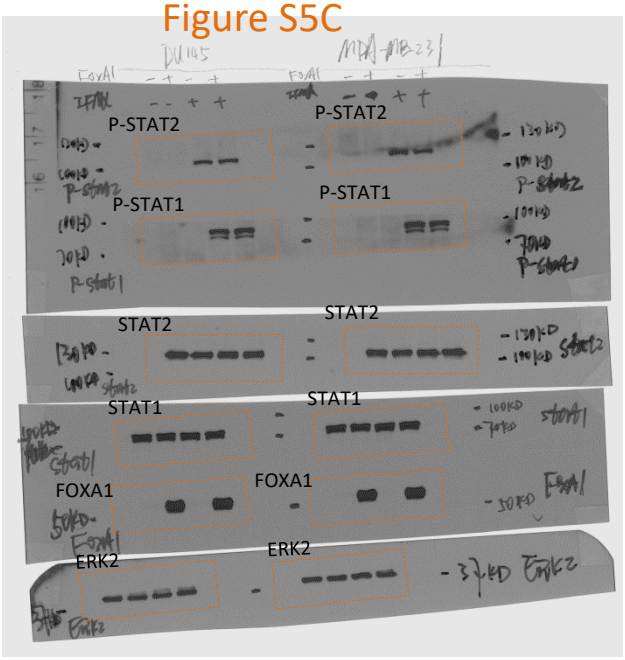

Figure S5D

Figure S5E

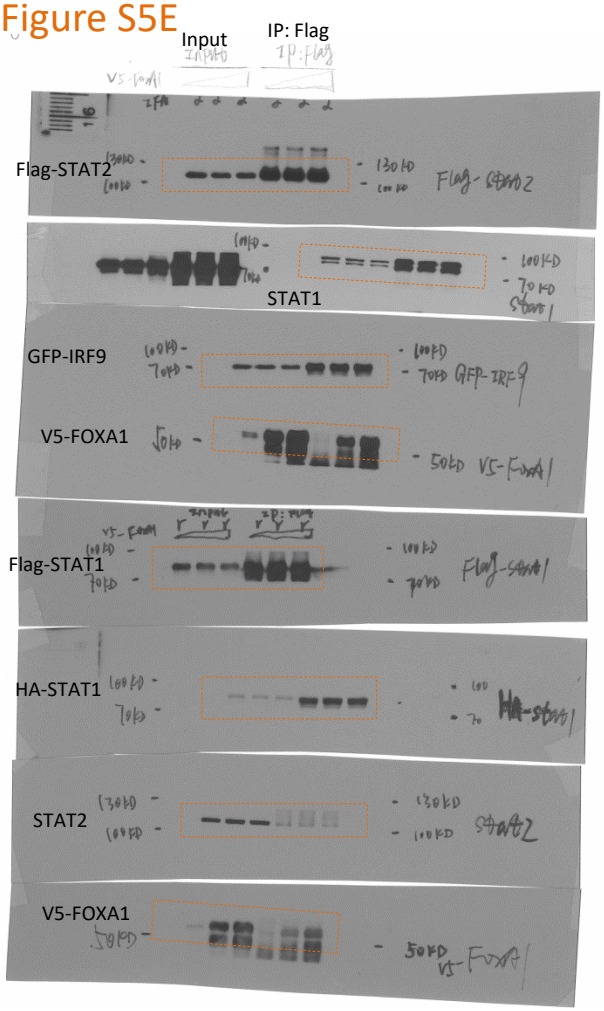

Figure S5F

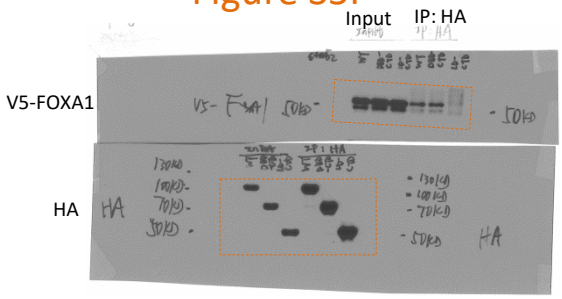

Figure S5G

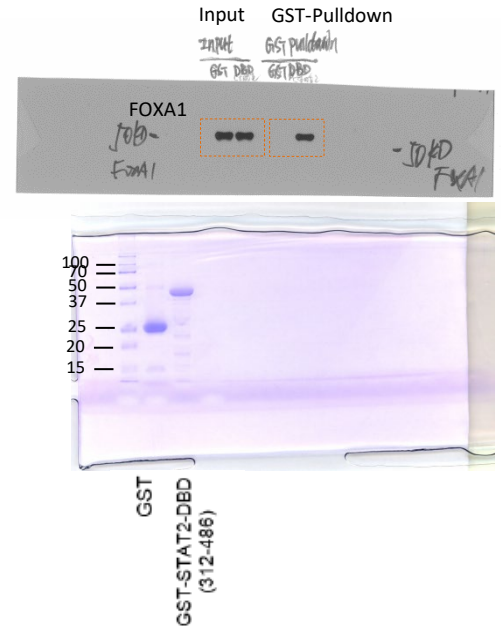

Figure S5H

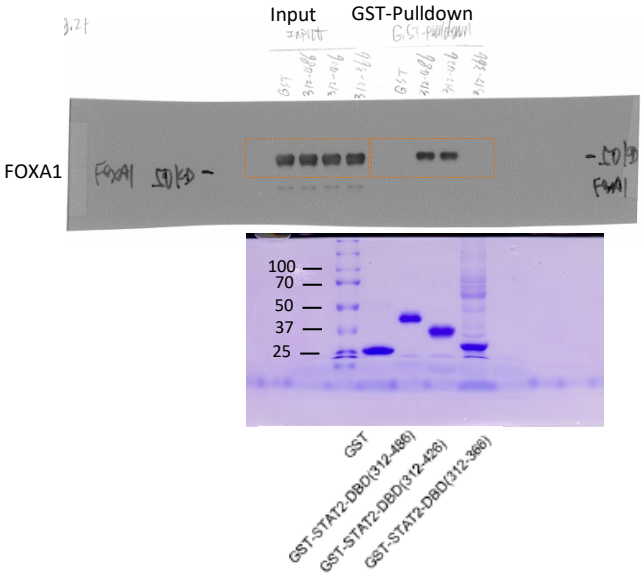

Figure 5I

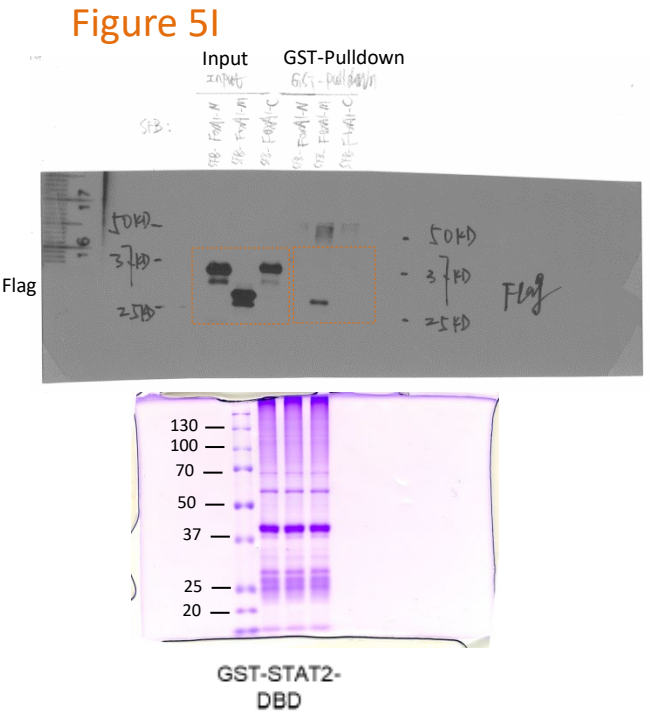

Figure S5J

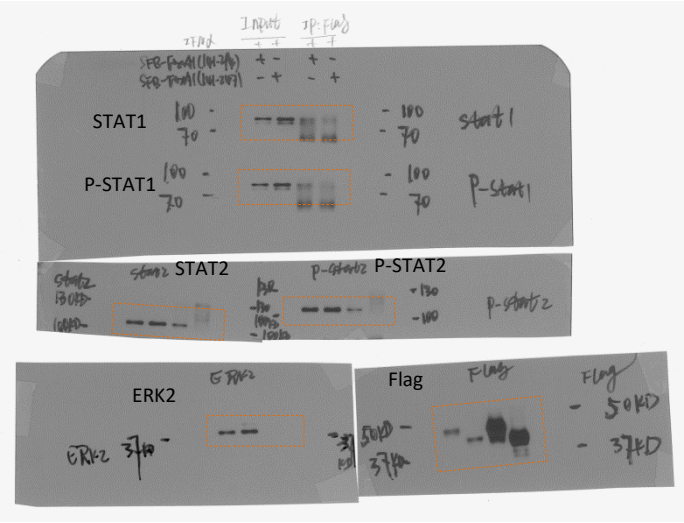

Figure S5L

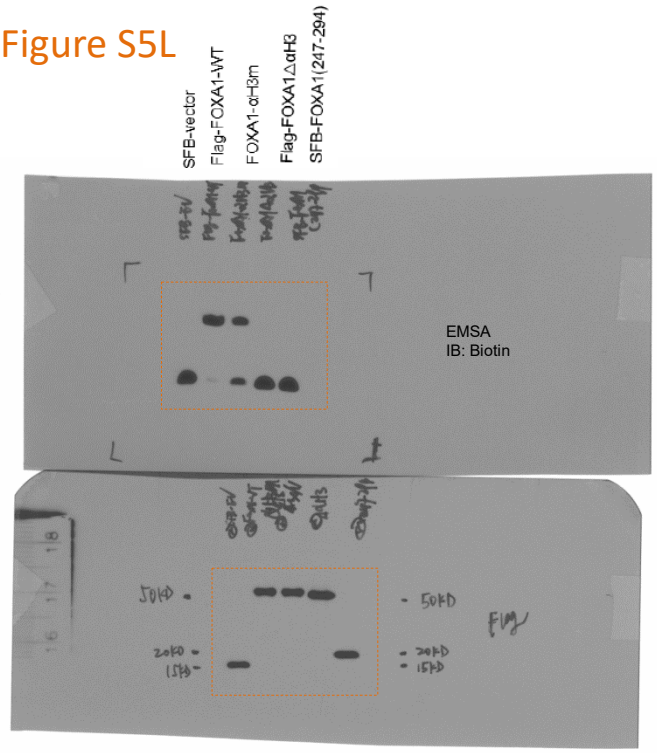

Figure S5N

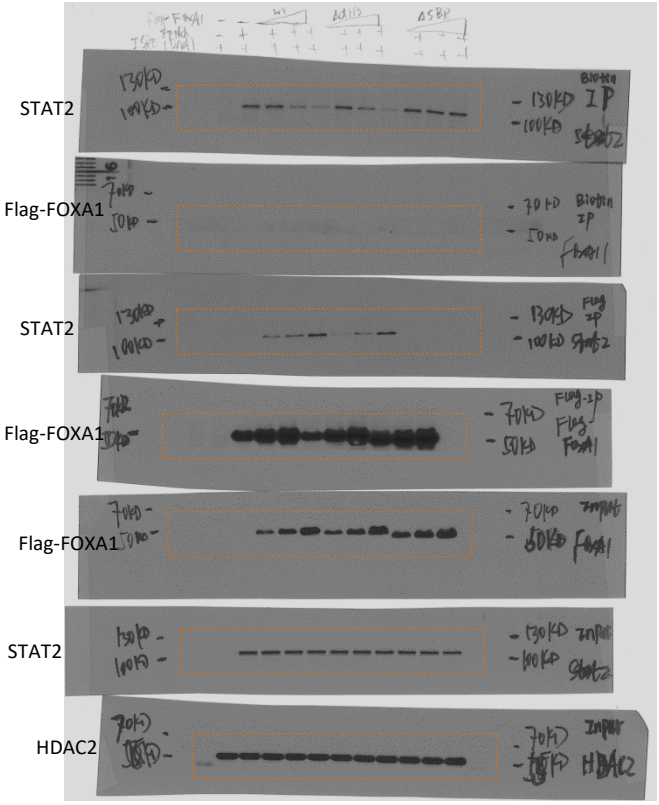

Figure S5O

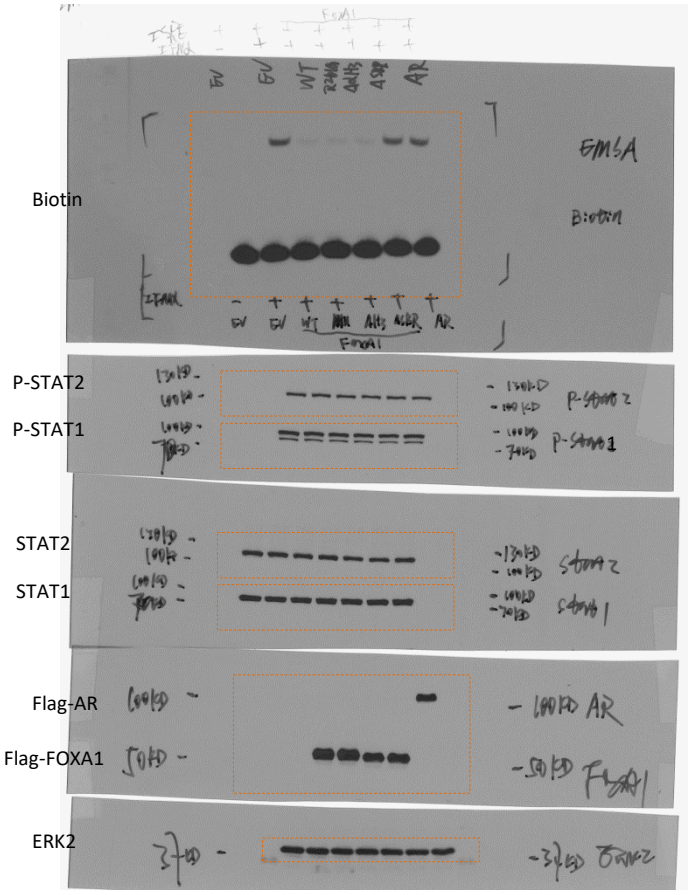

Figure S6A

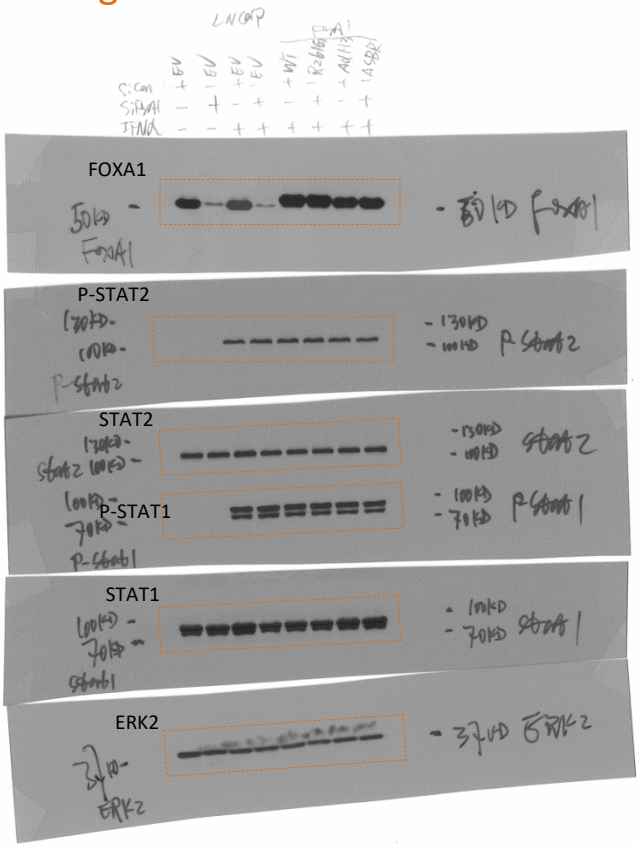

Figure S7B

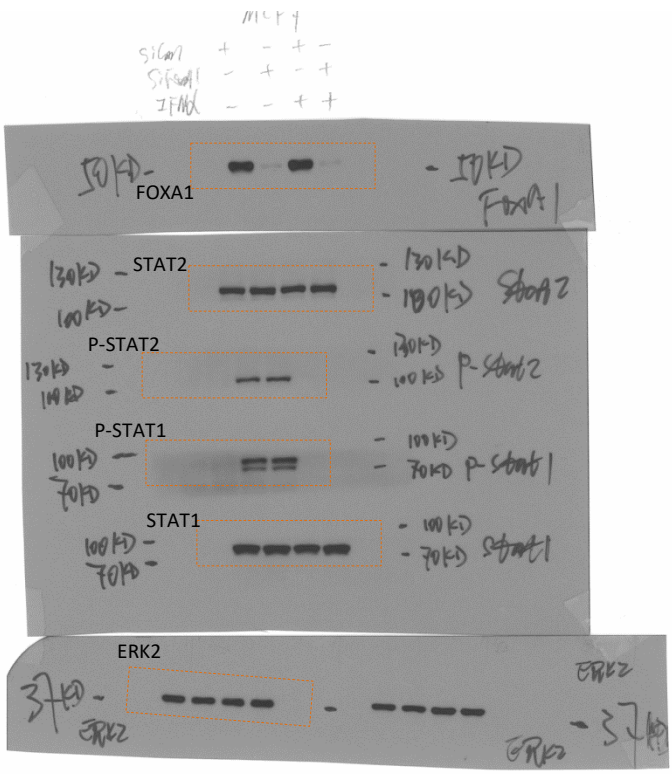

Figure S9A

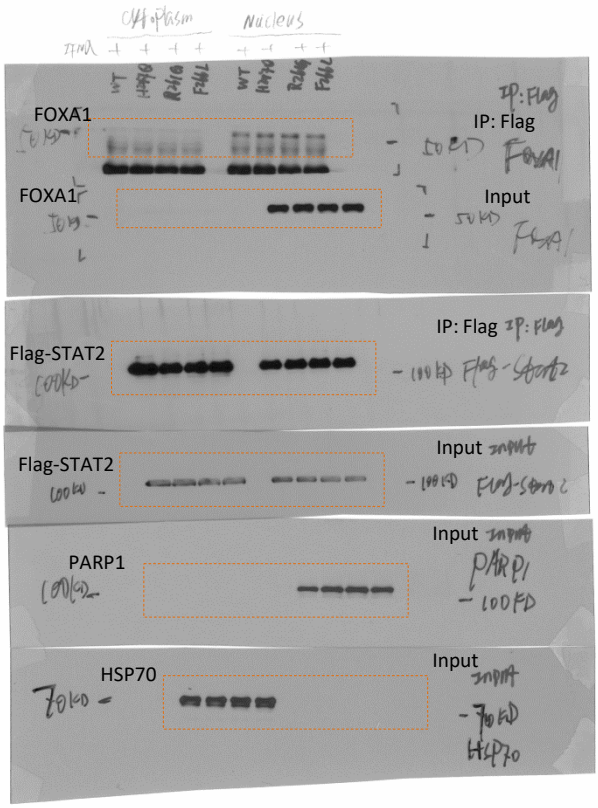

Figure S9B

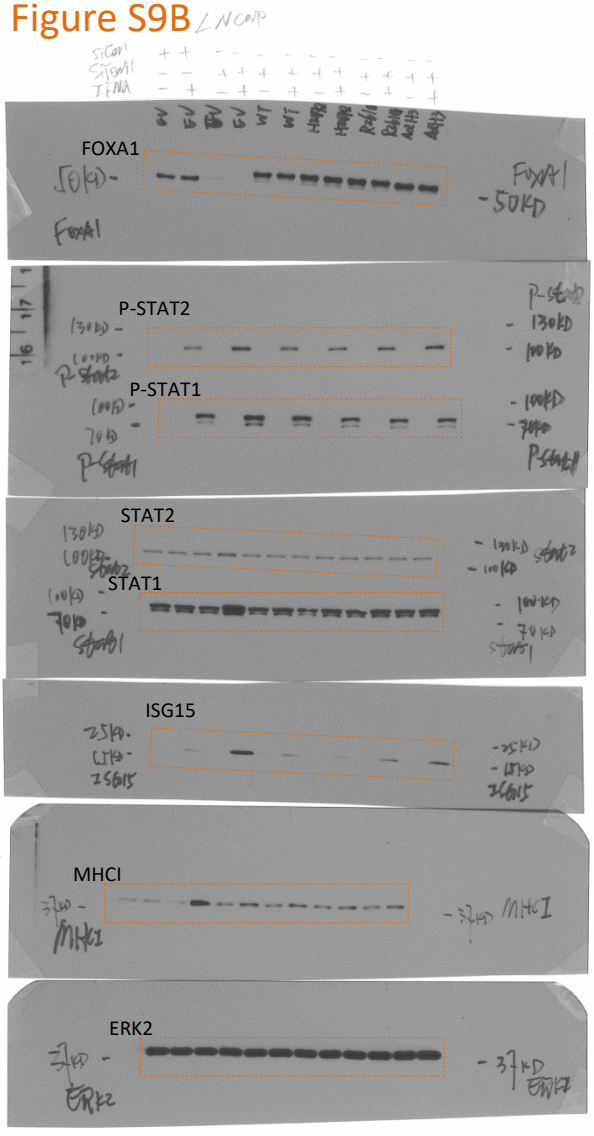

Figure S9C

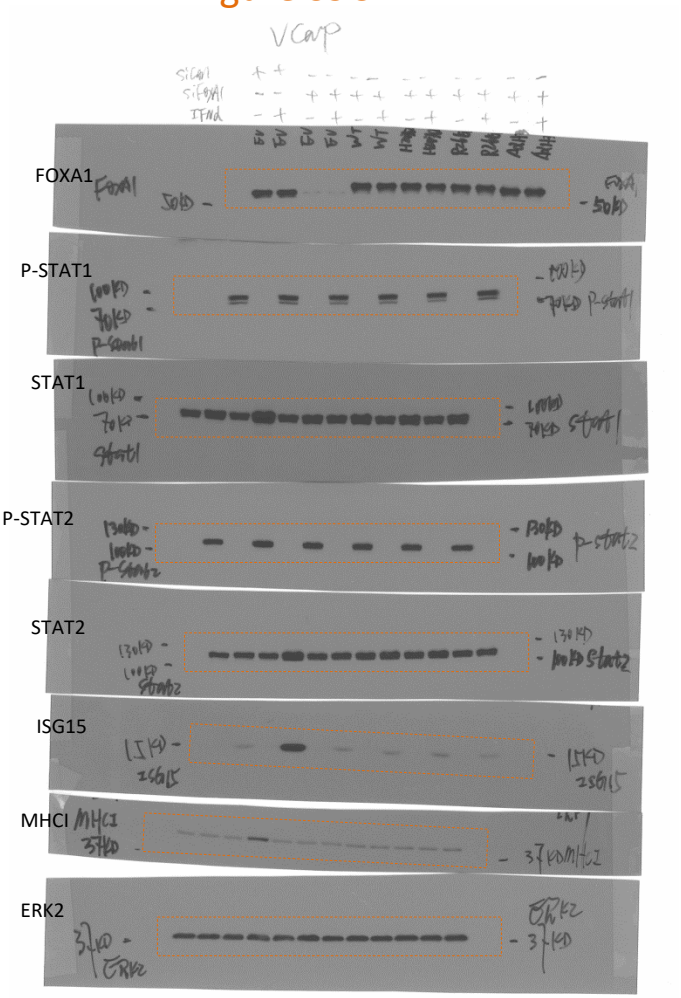

Figure S9D

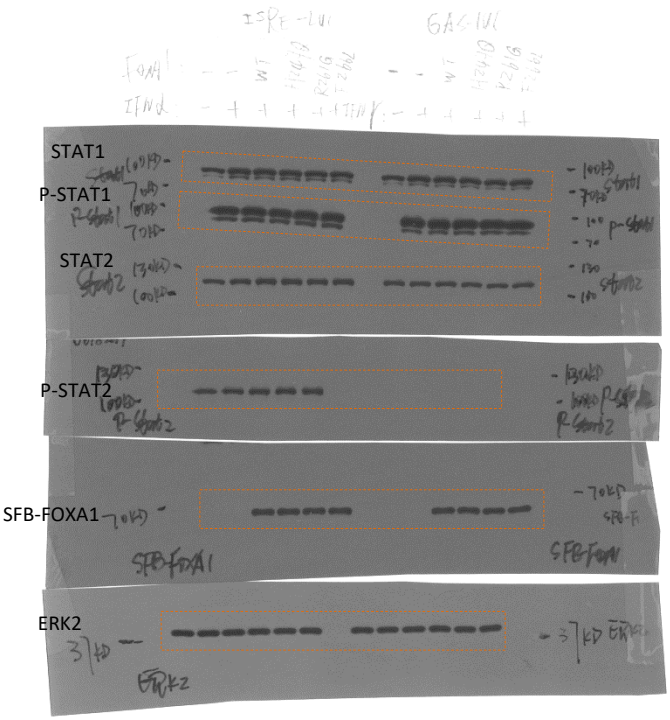

Figure S9H

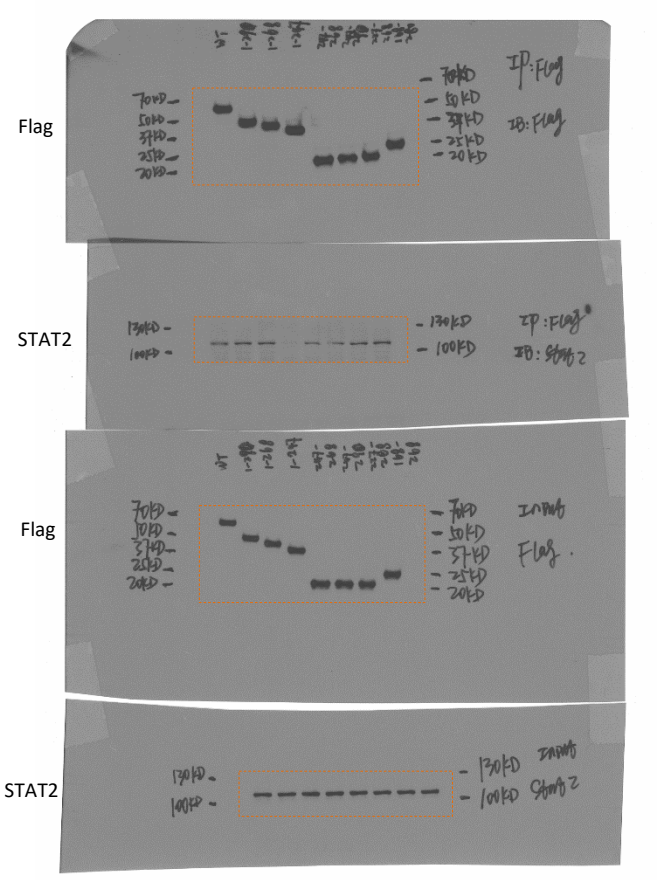

Figure S12A

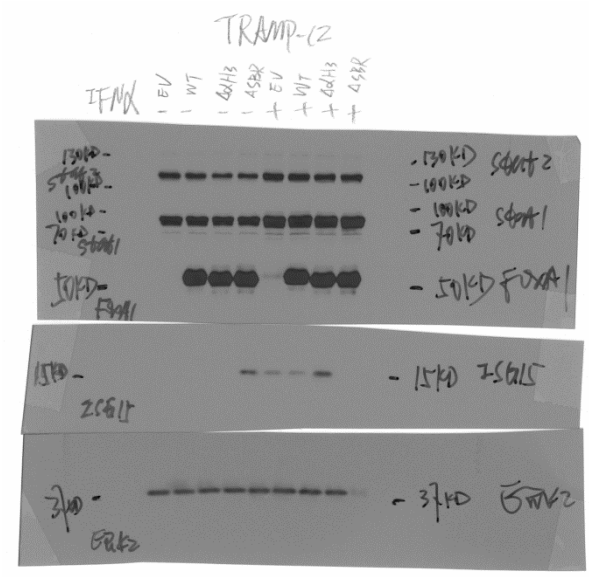

Figure S14B

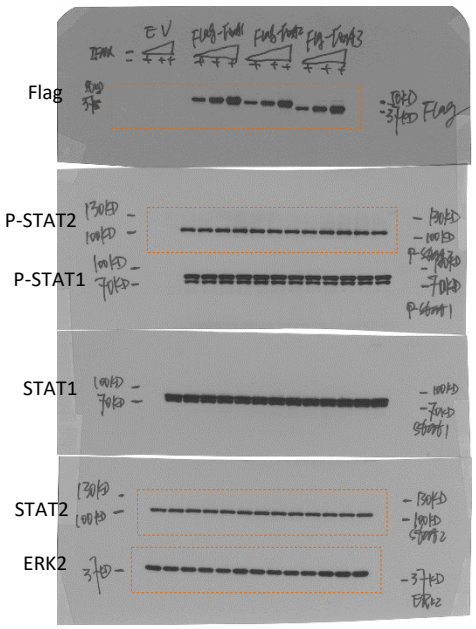

Figure S14C

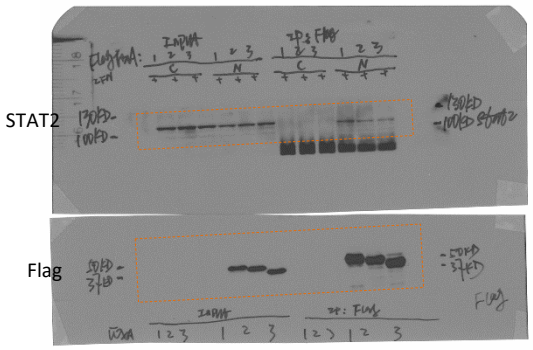

Figure S14D

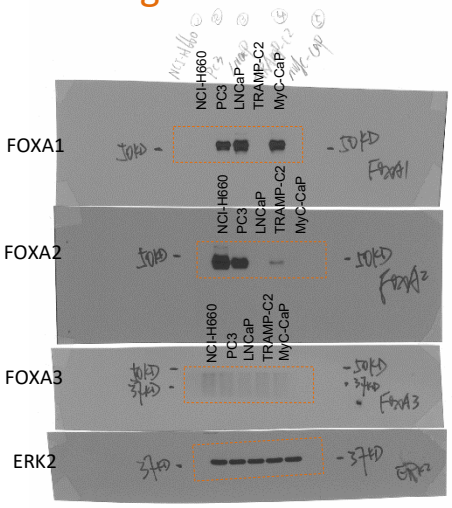

Figure S15A

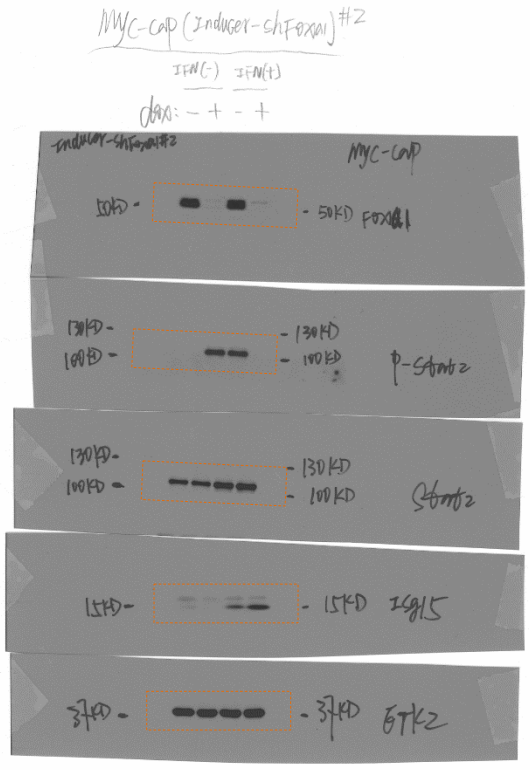

Figure S17A

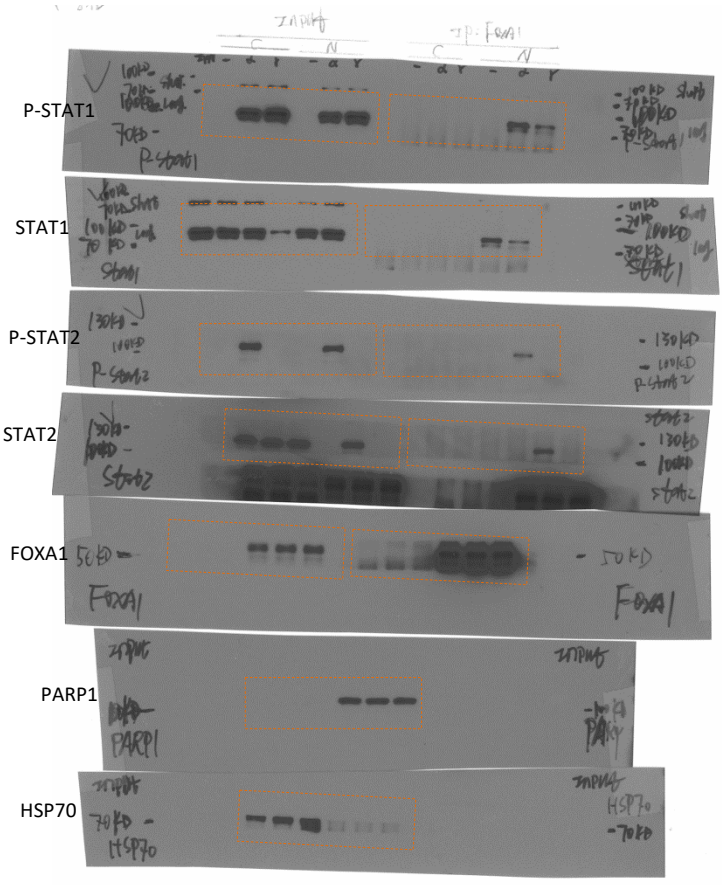

Figure S17B